

This is the accepted version of the manuscript published by Wiley in *European Journal of Neuroscience*, doi: 10.1111/ejn.13521

Bedwell¹, S. A., Billett, E. E., Jonathan J Crofts, J. J., & Tinsley, C. J. (2017). Differences in anatomical connections across distinct areas in the rodent prefrontal cortex. *European Journal of Neuroscience*, 55, 337–356.

Proposed Journal Section: Neurosystems

Title: Differences in Anatomical Connections across Distinct Areas in the Rodent Prefrontal Cortex

Running Title: Anterior-Posterior Organisation of PFC Connections

Authors: Stacey A Bedwell¹, E Ellen Billett¹, Jonathan J Crofts¹, Chris J Tinsley¹

Corresponding author: Stacey A. Bedwell - stacey.bedwell@ntu.ac.uk

Address #1:
School of Science and Technology
Nottingham Trent University
Clifton Lane
Nottingham
NG11 8NS

Number of figures: 12 Number of tables: 1 Number of words (abstract): 250 Number of words (introduction): 570 Number of words (whole manuscript): 6702

Keywords: cortical circuitry, temporal cortex, sensory-motor cortex, organization, tracing.

Conflicts of Interests:

The authors declare no conflict of interests

Author Contributions:

SAB performed the anatomical processing and analysed the data. SAB and CJT performed the experiments and wrote the manuscript. EEB, JJC and CJT co-designed the experiments and contributed to the choice of statistical analyses and EEB and JJC edited the manuscript.

Abstract

Prefrontal cortex (PFC) network structure is implicated in a number of complex higher-order functions and with a range of neurological disorders. It is therefore vital to our understanding of PFC function to gain an understanding of its underlying anatomical connectivity. Here, we injected Fluoro-Gold and Fluoro-Ruby into the same sites throughout rat PFC. Tracer injections were applied to two coronal levels within the PFC (anterior +4.7mm to bregma and posterior +3.7mm to bregma). Within each coronal level, tracers were deposited at sites separated by approximately 1mm and located parallel to the medial and orbital surface of the cortex. We found that both Fluoro-Gold and Fluoro-Ruby injections produced prominent labelling in temporal and sensory-motor cortex. Fluoro-Gold produced retrograde labelling and Fluoro-Ruby largely produced anterograde labelling. Analysis of the location of these connections within temporal and sensory-motor cortex revealed a consistent topology (as the sequence of injections was followed mediolaterally along the orbital surface of each coronal level). At the anterior coronal level, injections produced a similar topology to that seen in central PFC in earlier studies from our laboratory (i.e. comparing equivalently located injections employing the same tracer), this was particularly prominent within temporal cortex. However, at the posterior coronal level this pattern of connections differed significantly, revealing higher levels of reciprocity, in both temporal cortex and sensory-motor cortex. Our findings indicate changes in the relative organization of connections arising from posterior in comparison to anterior regions of PFC, which may provide a basis to determine how complex processes are organized.

Rat prefrontal cortex (PFC) is known to be crucially important in mediating a variety of cognitive (Alvarez and Emory, 2006; Fuster, 2001; Kolb, 1984; Schoenbaum and Roesch, 2005) and autonomic functions (Neafsey, 1990; Fryszak and Neafsey, 1994) yet it's anatomical structure is still not entirely described. In the rat brain prefrontal cortex is divided into distinct cytoarchitectural divisions within a broader grouping of medial and orbital PFC. Medial PFC includes the prelimbic (PL), infralimbic (IL) and anterior cingulate regions (Vertes, 2004; Vertes, 2006). Orbital PFC contains medial orbital (MO), ventral orbital (VO), ventral lateral orbital (VLO) and lateral orbital (LO) regions (Krettek and Price, 1977; Van De Werd and Uylings, 2008). The dorsal lateral orbital region (DLO) lies between LO and the agranular insular area (AI) (Van De Werd and Uylings, 2008). Medial PFC (mPFC) and orbital PFC are proposed to be functionally distinct (Schoenbaum and Roesch, 2005; Schoenbaum and Esber, 2010) and both regions are known to display different connections to other brain sites. Medial PFC is known to play important roles in the timing of motor behaviours (Narayanan and Laubach, 2006; Narayanan and Laubach, 2008; Narayanan and Laubach, 2009; Smith et al., 2010; Kim et al., 2013) and orbital PFC is proposed to provide information in terms of the expected outcomes of events (Schoenbaum and Esber, 2010; Schoenbaum and Roesch, 2005; Stalnaker et al., 2015).

Anatomical studies have reported topological projections from PFC to temporal and sensory-motor regions in rats (Sesack et al., 1989; Vertes, 2004; Hoover and Vertes, 2011; Kondo and Witter, 2014; Bedwell et al., 2014; Bedwell et al., 2015). Further topological connections have been reported in the projections from temporal cortex and sensory-motor cortex to PFC (Delatour and Witter, 2002; Bedwell et al., 2014; Bedwell et al., 2015; Reep et al., 1996). Ordering of connections from PFC to subcortical regions have also been described in the connections from PFC to the striatum (Berendse et al., 1992; Schilman et al., 2008). Taken together these studies provide strong evidence for topological PFC connections. Within a wider context of brain connectivity this is entirely consistent

because there is evidence that both sensory-motor cortex (Porter and White, 1983; Aronoff et al., 2010; Henry and Catania, 2006) and temporal cortex (Delatour and Witter, 2002; Arnault and Roger, 1990; Burwell et al., 1995) contain topographically arranged connections to other brain regions.

Typically, the topological ordering of PFC connections has often been described along the medial lateral axis. Changes in the organisation of rat cingulate PFC connections along the anterior-posterior (A-P) axis have also been identified (Olson and Musil, 1992). It is unclear whether or not this is a wider organisational principle also present in other regions, or what the precise functional relevance of such an organisation might be. However, it has been proposed that there are changes in cognitive processing characteristics, such as abstraction in anterior compared to posterior prefrontal cortex in humans (Taren et al., 2011).

The current study aimed to investigate how the organisation of connections changes between anterior and posterior PFC. The neuronal tracers Fluoro-Gold and Fluoro-Ruby were injected into regions of medial and lateral PFC (PL, VO, VLO and DLO, AI). We found that anterior and posterior PFC displayed topological connections to temporal and sensory-motor cortex. Our findings show that the topology observed and the relationship between input and output connections changes between anterior and posterior PFC regions, this was clearest in the connections to temporal cortex.

Experimental Procedures

Data was collected from 18 male CD rats (296-367g, Charles River, UK). Animal procedures were carried out in accordance with the UK Animals scientific procedures act (1986), EU directive 2010/63 and were approved by the Nottingham Trent University Animal Welfare and Ethical Review Body. On receipt the animals were examined for signs of ill-health or injury. The animals were acclimatized for 10 days during which time their health status was assessed. Prior to surgery the animals were

housed together in individually ventilated cages (IVC; Techniplast double decker Greenline rat cages). The animals were allowed free access to food and water. Mains drinking water was supplied from polycarbonate bottles attached to the cage. The diet and drinking water were considered not to contain any contaminant at a level that might have affected the purpose or integrity of the study. Bedding was supplied by IPS Product Supplies Ltd in the form of 8/10 corncob. Environmental enrichment was provided in the form of wooden chew blocks and cardboard fun tunnels (Datesand Ltd., Cheshire, UK). Post-surgery the animals were individually or pair housed in the same conditions. The animals were housed in a single air-conditioned room within the Biological support facilities barrier unit, Nottingham Trent University. The rate of air exchange was at least fifteen air changes per hour and the low intensity fluorescent lighting was controlled to give 12 h continuous light and 12 h darkness. The temperature and relative humidity controls were set to achieve target values of $21 \pm 2^{\circ}\text{C}$ and $55 \pm 15\%$ respectively.

Individual bodyweights were recorded on Day - 10 (prior to the start of dosing) and daily thereafter. All animals were examined for overt signs of ill-health or behavioral change immediately prior to surgery dosing, during surgery and the period following surgery. There were no observed clinical signs/symptoms of toxicity or infection. There was no significant effect on body weight development detected.

Rats were anaesthetized with isoflurane (Merial, Harlow, UK) and placed in a stereotaxic frame with the incisor bar set so as to achieve a flat skull. Buprenorphine (0.05 mg/kg i.m/s.c) and Meloxicam (up to 1 mg/kg s.c/orally) analgesia were provided peri-operatively and for several days post-operatively. Body temperature was monitored during and immediately after surgery using a rectal thermometer. Craniotomies (<1 mm) were made at predetermined stereotaxic coordinates. Sterile tracer solution was deposited into the PFC via a 0.5 μl neuro-syringe (Hamilton, Germany).

Injections of anterograde (10% Fluoro-Ruby in distilled water, Fluorochrome, Denver, Colorado (10 nl/min, 2 min diffusion time)) and retrograde tracer (4% Fluoro-Gold in distilled water, Fluorochrome, Denver, Colorado (100 nl/min, 2 min diffusion time)) were targeted at anterior and posterior PL, VO, VLO or DLO/AI with the intention of revealing the anatomical connections of prefrontal regions. The distance between craniotomy co-ordinates (1 mm) was based on the measured spread of tracers in preliminary and previous studies (<1 mm in diameter). Craniotomies were repeated at 2 anterior-posterior levels (+4.2mm and +3.2mm from Bregma) – see full list of animals and corresponding injection sites in table 1. The medial-lateral co-ordinates and depth of injections below the cortical surface at the anterior and posterior levels are shown in Figure 1. Figure 1 shows that the histological assessed locations of the injections differed slightly from the surgical coordinates, i.e. the anterior and posterior injections were assessed as occurring at +4.7mm and +3.7mm with respect to bregma and following the atlas of Paxinos and Watson, 1998. The coordinates were chosen to avoid the sagittal sinus of the forebrain.

Each rat received injections of Fluoro-Ruby (100nl) and/or Fluoro-Gold (100nl) into various subdivisions of PFC, separated by 1 mm and at an angle of 0 degrees from vertical in the medial-lateral and anterior-posterior axes. Rats received an injection of Fluoro-Gold into one hemisphere and an injection of Fluoro-Ruby into the other hemisphere, to allow accurate identification of the tracers injected. Further dual injections of Fluoro-Gold and Fluoro-Ruby were targeted at anterior and posterior VO and DLO/AI. This was performed to test whether the different projections arising from anterograde or retrograde tracer injections into these regions (and notably to the temporal cortex region), were not due differences in the injections sites of the single tracer injections. Dual injections were made via a first injection of Fluoro-Gold, followed by a second injection of Fluoro-Ruby into the same injection site.

Following a survival time of 7–9 days, the rats were deeply anesthetized with pentobarbital (Sigma-Aldrich, UK), and transcardially perfused with phosphate buffered saline (PBS) (pH 7.4) (~200 ml) followed by 4% paraformaldehyde (PFA) (pH 7.4) (~200 ml). The brain was subsequently removed and stored for 24 h in 4% PFA in PBS (pH 7.4), followed by cryoprotection in 30% sucrose in PBS.

Anatomical processing

For analysis of connections, two series of 40µm coronal sections were taken (2 in 6 sections) on a freezing microtome (CM 1900, Leica, Germany). Sections were mounted onto gelatin coated slides. The first series was cover slipped with Vectashield® mounting medium (with propidium iodide) for fluorescent imaging of Fluoro-Gold (for the injection and projection site). A parallel series of 40µm coronal sections was cover slipped with Vectashield® mounting medium (with DAPI) for fluorescent imaging of Fluoro-Ruby (for the injection and projection site).

Sections were examined using fluorescent microscopy (Fluoro-Ruby and Fluoro-Gold). Fluorescent photos were captured of the injection sites and the anterograde and retrograde labelling using an Olympus DP-11 system microscope with a x4, x10 and x20 objective lens.

Immunofluorescent staining of alpha tubulin with fluorescein enabled us to visualize where Fluoro-Ruby labelling occurred in relation to cell bodies, thus establishing the anterograde/retrograde nature of Fluoro-Ruby. Alpha-Tubulin was labelled in several animals R37, R38 and R39. Sections were incubated in an alpha-tubulin monoclonal primary antibody (sc-398103, Santa Cruz, TX) at a dilution of 1:50 overnight at 4°C and secondary antibody (Fluorescein Horse Anti-Mouse IgG Antibody, Vector Laboratories, UK (in PBS, 2% NS) at a dilution of 1:75 for 1-2 hours. Fluorescein stained sections were cover-slipped with Vectashield® mounting medium (with DAPI) for fluorescent

imaging. Fluoro-Ruby labels, DAPI stained nuclei and fluorescein stained α -Tubulin were visualized at a high resolution using confocal microscopy.

Microscopic analysis

The entire forebrain was examined for afferent and efferent connections. Areas of temporal and sensory-motor cortex were found to contain the strongest and most consistent labelling of connections from anterior and posterior PFC. A more detailed analysis was carried out on these regions to examine the organisation of connections across PFC.

Alpha-tubulin and Fluoro-Ruby labelling was visualised with confocal microscopy. A Z-series of images was taken at X10, X20 and X40 magnification in sequential scanning mode for each channel using Leica confocal software (LAS AF). Step size between consecutive sections was 1.5 μ m. In total 13 images were taken for each section, across 20.5 μ m. Each maximal image was composed of multiple sections to ensure optimum capture of the fluorescent tracers/stains.

ImageJ (Wayne Rasband, NIH) was used to determine numerical values representing the location of retrograde and anterograde labelling in temporal and sensory-motor cortex in 3 dimensional coordinates, x, y and z. The dorsoventral and medial-lateral distance (i.e. laminar location) of each Fluoro-Gold labelled cell in temporal cortex was measured from the rhinal sulcus and cortical surface respectively (in mm). The anterior-posterior location of each retrogradely labelled cell in temporal cortex was also recorded, in terms of distance (mm) from Bregma according to a stereotaxic atlas (Paxinos and Watson, 1998). This process was repeated for Fluoro-Ruby labelling where anterograde axon terminals were usually located close to the cell membrane of neuronal cell soma. A similar acquisition of data was implemented for afferents/efferents in sensory-motor cortex, whereby the dorsoventral and medial-lateral distance of retrograde cells/axon terminals from the cortical surface

was recorded (dorsoventral distance was measured from the dorsal aspect of the cortical surface and the medial-lateral measurement was recorded as the distance from the midline). The anterior-posterior location of each retrograde/anterograde marker in sensory-motor cortex was also recorded, in terms of distance (mm) from Bregma. The position of all the individual afferent/efferent labelling associated with an individual tracer injection were recorded and the x, y and z values were calculated as a mean for each injection.

Statistical Analyses

Retrograde labelled cells or afferent axon terminal positions were grouped according to injection site location and the positional data was found to be normally distributed. The data sets were analysed with 2 factor ANOVA (injection site, tracer) using SPSS (IBM) to verify the effect of injection location on positioning of labelled cells in anterior-posterior, dorsoventral and medial-lateral dimensions. All statistical tests were applied with a significance level of 0.05 and confidence intervals of 95%.

Results

Fluoro-Gold afferents were found in areas of primary and secondary motor cortex (M1, M2), primary somatosensory cortex (jaw region and barrel field - S1J, S1BF), area 1 of cingulate cortex (Cg1), piriform cortex (Pir), perirhinal cortex (PRh - areas 35v, 35d, 36d, 36v), entorhinal cortex (Ent), primary auditory cortex (Au1), ventral secondary auditory cortex (AuV) and prefrontal regions.

Fluoro-Ruby labelling was found in areas of M2, S1J, Cg1, S2, PRh, Ent, dorsal agranular insular cortex (AI) and prefrontal regions. The organisation of input and output connections was investigated separately at two anterior-posterior PFC locations (anterior (4.7mm from Bregma) and posterior (3.7mm from Bregma)).

Injections into anterior and posterior PFC

Fluoro-Gold injection sites in the anterior (bregma + 4.7mm) and posterior (bregma +3.7mm) aspect of PFC were observed in PL, VO, VLO and DLO anteriorly, and in PL, Cg1, IL, MO, VO, VLO, LO, AI, Dysgranular insular areas (DI) and Granular Insular cortex (GI) posteriorly (Figure 1ii, iv). These injection sites were mostly confined to layers I-V/VI. No overlapping occurred between Fluoro-Ruby PFC injection sites. Fluoro-Ruby injection sites were observed in PL, Frontal Association (FrA), VO, VLO and DLO anteriorly and in PL, Cg1, IL, MO, VO, VLO, LO, AI, DI and GI posteriorly (Figure 1ii, iv).

Anterior PFC: There was some overlap seen between the Fluoro-Gold injection sites in PL (R28) and VO (R24). There was some minimal overlap between the Fluoro-Gold injections into VO/MO and VLO (R24 and R17). The dorsal medial Fluoro-Gold injection occurred primarily within PL (with a lesser presence in MO and VO) and the ventral medial injection occurred within VO and also MO and PL (R28 and R24). The more central injection was primarily located within VLO. The most lateral Fluoro-Gold injection occurred within DLO₂, but also occupied parts of DLO₁ and LO. Fluoro-Ruby injection sites into anterior PFC were observed in similar regions to the equivalent Fluoro-Gold injection sites, the spread of Fluoro-Ruby injections was consistently contained within the boundary of Fluoro-Gold counterparts. The dorsal medial Fluoro-Ruby injection occurred within PL and the ventral medial injection occurred within VO (R32 and R21). The more central injection was primarily located within VLO with spread into FrA, and the most lateral Fluoro-Ruby injection was primarily located within DLO₂, with some overlap into DLO₁. The Fluoro-Gold injections were typically more tear-drop shaped than the Fluoro-Ruby injections, i.e. their horizontal spread was greater. In addition to the single injections, dual injections of tracer (Fluoro-Gold and Fluoro-Ruby) were deposited at the same lower medial and lateral injection sites. The position and spread of these tracers closely

matched those of the corresponding Fluoro-Gold single injections (see also Figure 1i). In subsequent figures these injections are referred to PL, VO, VLO and DLO (or arbitrarily denoted Aa, Ba, Ca and Da) because the primary site of these injections was in the targeted site.

Posterior PFC: The dorsal medial Fluoro-Gold injection into PL (R27) spread across layers II-VI and overlapped slightly with the injections targeting VO and VLO (R22 and R11). This injection occupied PL, Cg1 and M2. The ventral medial injection targeting VO (R22) overlapped with the PL injection (R27) and spread into IL and PL, however the majority of injected tracer was seen within the intended regions of VO and MO. The central orbital, VLO injection site also spread beyond the intended region (into M2), however the majority of injected tracer remained within the boundaries of VLO and covered layers I-VI (R11). The lateral injection site did not overlap with any other Fluoro-Gold injection sites, and was centered within the cytoarchitectural region of LO and AI (with some spread into DI and GI) (R26). All of the Fluoro-Ruby injection sites produced a smaller spread of tracer than the corresponding Fluoro-Gold injection sites. The dorsal medial Fluoro-Ruby injection occupied both PL and Cg1 and the ventral medial injection was located within MO, IL and PL (R28 and R26). The central orbital Fluoro-Ruby injection was located in VLO (R25) and the lateral orbital injection was in DLO₂ and DLO₁ (R27). Additional dual injections of tracer (Fluoro-Gold and Fluoro-Ruby) were deposited at the same ventral medial and lateral injection sites. The spread of these tracers closely resembled the equivalent Fluoro-Gold single injections but was slightly more extensive in the case of the ventral medial injection (as far as just inside VLO) and (Figure 1ii).

Afferent/Efferent labelling following PFC tracer injections

Fluoro-Gold afferents, resultant from tracer injections into anterior (+4.7mm from Bregma) PFC were found in regions of PRh (36v, 36d, 35d), Ent, AuV, Cg1, M2, M1, S1J and prefrontal regions (Figure 2i, Figure 3i). Fluoro-Ruby efferents resultant from tracer injections into the same co-ordinates in

anterior PFC were found in regions of PRh (36v, 36d, 35d), Ent, Cg1, M2 and M1, as well as prefrontal regions (Figure 2iv, Figure 3iv).

Fluoro-Gold afferents, resultant from injections into posterior (+3.7mm from Bregma) PFC were found in regions of PRh (35v, 35d, 36v, 36d), Ent, AuV, Cg1, M2, M1, S1J and prefrontal regions (Figure 2ii, Figure 3ii). Fluoro-Ruby axon terminals resultant from injections into posterior PFC were found in regions of PRh (35d, 36v, 36d), Ent, Cg1, M2 and M1, as well as prefrontal regions (Figure 2iv, Figure 3iv).

We also wanted to verify the location of the peri-cellular labelling of Fluoro-Ruby within the projection fields. Immunofluorescent imaging of alpha-tubulin alongside Fluoro-Ruby labelling in temporal cortex indicated that the majority (70%) of Fluoro-Ruby labelling we observed in temporal cortex, as a result of injections into prefrontal cortex, was separate from the fluorescein labelled (i.e. alpha-tubulin stained), cell bodies (Figure 4). There was some evidence of double labelling of alpha tubulin and Fluoro-Ruby (Figure 4), approximately 30% of cases were found to have retrograde properties (i.e. Fluorescein and Fluoro-Ruby labelling were seen in the same location).

Organisation and distribution of connections from Anterior PFC to Temporal Cortex

The distribution of retrograde labelled neurons in temporal cortex maintained a topology in terms of the corresponding Fluoro-Gold anterior PFC injection site. Moving from medial to lateral in PFC (from MO/VO to DLO), projections were seen more posteriorly within temporal cortex (fig 5i).

The distribution of anterograde efferents (from Fluoro-Ruby) in temporal cortex resultant from anterior PFC tracer injections was less widespread than the corresponding retrograde afferents (from Fluoro-Gold) (Figure 5iii). The distribution and topology of Fluoro-Ruby connections also differed

to the distribution of Fluoro-Gold projections. Although the labelling appeared in the same extent of temporal cortex the Fluoro-Ruby injections produced orbital projections (moving medial to lateral, MO/VO-DLO) at broadly progressively anterior locations within temporal cortex. The clearest differences in the locations of anterograde and retrograde labelling resulted from injections into both VO and DLO.

The distribution of anterior prelimbic projections to temporal cortex did not appear to follow a topology consistent with the other orbital PFC sites: i.e. with retrograde labels in temporal cortex becoming more ventrally and posteriorly positioned as injection sites in PFC moved from medial to lateral; and with anterograde labels becoming more anteriorly located as injection sites in PFC moved from medial to lateral. The projections arising from anterior prelimbic injections fell within this range of distributions rather than outside of it. The retrograde Fluoro-Gold afferents occurred in a similar temporal cortex region as the central orbital injections, i.e. VLO (Fig 5i). The anterograde, Fluoro-Ruby efferents occurred in a similar temporal cortex region to the area labelled following injections into the central orbital region (Fig 5iii).

Statistical analysis of the location of retrograde and anterograde projections produced the following results: A two factor ANOVA (injection site [dorsal medial, ventral medial, central orbital, lateral], tracer [Fluoro-Gold, Fluoro-Ruby]) revealed a significant main effect of anterior PFC injection site (single and dual injections) on labelling in temporal cortex in the dorsal-ventral ($F_{(3,1200)}=10.003$ $p<.001$), anterior-posterior ($F_{(3,1200)}=120.047$ $p<.001$) and medial-lateral ($F_{(3,1200)}=365.983$ $p<.001$) axes. Significant interaction effects of tracer*injection site on temporal cortex labelling were found in the dorsal-ventral ($F_{(3,1200)}=5.512$ $p=.001$), anterior-posterior ($F_{(3,1200)}=329.570$ $p<.001$) and medial-lateral ($F_{(3,1200)}=204.578$ $p<.001$) axes. The effect of injection site shows that the injection position effects the location of the projections. The significant interaction reveals that the afferent and efferent projections occurred at different locations over the injection sites investigated.

Organisation and distribution of Connections from Posterior PFC to Temporal Cortex

The distribution of retrograde cells within temporal cortex maintained a topological distribution according to the corresponding Fluoro-Gold posterior PFC injection sites. Moving from medial to lateral in posterior PFC (from MO/VO to AI), afferents were seen at progressively anterior locations within temporal cortex. For example, retrograde cells resultant from VO (and MO,IL,PL) injection were most posteriorly located, and VLO (and M2) injection produced labelling in more anteriorly located temporal cortex sites (fig.5ii).

The distribution of anterograde efferents maintained a topology according to Fluoro-Ruby posterior PFC injection sites which was similar to that for retrograde neurons (Figure 5iv). This was not fully the case for VO, where anterograde labelling was seen in a similar region to equivalent retrograde labelling, in addition to a more anterior location. Moving from medial to lateral in posterior PFC (MO/VO to AI), anterograde terminals in temporal cortex occurred at increasingly anterior locations (fig.5iv). In contrast to anterior PFC, injections at equivalent mediolateral injections (i.e. 1.2, 2.2 or 3.3mm lateral to the midline) produced similar locations for anterograde and retrograde projections within temporal cortex.

The distribution of posterior prelimbic projections to temporal cortex also did not appear to follow the topological organisation of the other, orbital PFC sites. The Fluoro-Gold label occurred in a relatively anterior temporal cortex location compared to the orbital injections (Fig 5ii). The anterograde, Fluoro-Ruby label again occurred in a similar temporal cortex region to the area labelled following injections into the central orbital region (Fig 5iv).

Statistical analysis of the location of retrograde and anterograde projections produced the following results: A two factor ANOVA (injection site, tracer) revealed a significant main effect of posterior PFC injection site (single and dual injections) on labelling in temporal cortex in the anterior-posterior ($F_{(3,1090)}=394.975$ $p<.001$) and medial-lateral ($F_{(3,1090)}=28.494$ $p<.001$) axes but not in the dorsal-ventral axis ($F_{(3,1090)}=.720$ $p=.540$). Significant interaction effects of tracer*injection site on temporal cortex labelling were found in the dorsal-ventral ($F_{(3,1090)}=3.652$ $p=.012$), anterior-posterior ($F_{(2,1090)}=141.767$ $p<.001$) and medial-lateral ($F_{(3,1090)}=25.053$ $p<.001$) axes.

Organisation and distribution of Connections from Anterior PFC to Sensory-motor cortex

The distribution of retrograde cells in sensory-motor cortex maintained a topology according to the corresponding (Fluoro-Gold) anterior PFC injection sites (VO, VLO and DLO). Moving from medial to lateral in PFC (from MO/VO to DLO), projections were seen more posteriorly within sensory-motor cortex (fig 6i).

The distribution of anterogradely labelled axon terminals in sensory-motor cortex maintained a different topology in terms of the corresponding Fluoro-Ruby anterior PFC injection site (Fig.6iii). Moving from medial to lateral in PFC (from MO/VO to DLO), this time projections were seen at increasingly anterior locations. For example, connections from VLO (and M2) were seen at more anterior locations compared to those arising from VO. The VO and DLO injection sites had the most different locations of anterograde efferents and retrograde afferents within sensory-motor cortex.

The distribution of anterior prelimbic projections to sensory-motor cortex did not appear to follow the topological organisation of the other orbital PFC sites. The retrograde Fluoro-Gold afferents occurred in a similar sensory-motor cortex region as the central orbital injections, i.e. VLO (Fig 6i).

The anterograde Fluoro-Ruby efferents again occurred in a similar sensory-motor region to the area labelled following injections into the lateral orbital region, i.e. DLO (Fig 6iii).

Statistical analysis of the location of retrograde and anterograde projections produced the following results: A two factor ANOVA revealed a significant main effect of anterior PFC injection site (single and dual injections) on labelling in sensory-motor cortex in the dorsal-ventral ($F_{(3,1265)}=75.39$ $p<.001$), anterior-posterior ($F_{(3,1265)}=4.762$ $p=.003$) and medial-lateral ($F_{(3,1265)}=268.462$ $p<.001$) axes. Significant interaction effects of tracer*injection site on sensory-motor cortex labelling were found in the dorsal-ventral ($F_{(3,1265)}=145.429$ $p<.001$), anterior-posterior ($F_{(3,1265)}=116.496$ $p<.001$) and medial-lateral ($F_{(3,1265)}=144.380$ $p<.001$) axes.

Organisation and distribution of connections from Posterior PFC to Sensory-motor cortex

The distribution of retrograde cells within sensory-motor cortex maintained some topological ordering according to the corresponding Fluoro-Gold injection sites in posterior PFC. Moving laterally in PFC from MO/VO to AI: projections were seen more anteriorly within sensory-motor cortex (fig 6ii). Here afferents from the injection into VO, MO, IL and PL (denoted Bp) and LO, AI, DI and DG (denoted Dp) were located anteriorly to that resulting from injection into VO.

The distribution of anterograde, axon terminals in sensory-motor cortex maintained a topology corresponding to Fluoro-Ruby posterior PFC injection sites, which resembled that of Fluoro-Gold afferents. As PFC injection sites move from medial to lateral (MO/VO to AI), efferents in sensory-motor cortex occurred at increasingly anterior locations (fig.6iv). In contrast to anterior PFC, the VO, MO, IL and PL (denoted Bp) and LO, AI, DI and DG (denoted Dp) injection sites had similar locations of anterograde and retrograde labelling within temporal cortex.

The distribution of posterior prelimbic projections to sensory-motor cortex did not appear to follow a topology consistent with the other orbital PFC sites. The retrograde Fluoro-Gold afferents occurred in a similar sensory-motor cortex region as the central orbital injections, i.e. VLO/M2 (Fig 6ii). The anterograde, Fluoro-Ruby, efferents again occurred in a similar sensory-motor region to the area labelled following injections into the lateral orbital region, i.e. injection Dp: LO, AI, DI, GI (Fig 6iv).

Statistical analysis of the location of retrograde and anterograde projections produced the following results: A two factor ANOVA revealed a significant main effect of posterior PFC injection site (single and dual injections) on labelling in sensory-motor cortex in the dorsal-ventral ($F_{(3,1293)}=75.833$ $p<.001$), anterior-posterior ($F_{(3,1293)}=234.566$ $p<.001$) and medial-lateral ($F_{(3,1293)}=63.283$ $p<.001$) axes. Significant interaction effects of tracer*injection site on sensory-motor cortex labelling were found in the dorsal-ventral ($F_{(3,1293)}=123.547$ $p<.001$), anterior-posterior ($F_{(3,1293)}=4.615$ $p=.003$) and medial-lateral ($F_{(3,1293)}=64.4$ $p<.001$) axes.

Results from dual injections into VO and DLO/AI

One of the clearest results of our study was the finding that our anterior anterograde or retrograde tracer injections into VO or DLO resulted in a different distribution of tracer terminations, notably within the temporal cortex. To test whether this resulted from the differences in actual injection sites achieved by single injections we targeted the same sites with dual injections of Fluoro-Gold and Fluoro-Ruby. Fluoro-Gold and Fluoro-Ruby labelling resultant from dual tracer injections targeted at anterior VO and DLO and posterior VO and AI was seen in similar regions to that observed from equivalent single injections (figures 7 & 8). Furthermore, following dual injections we observed essentially the same organizational pattern of connections: that injections into either anterior VO or DLO resulted in FG and FR labelling in different locations. In comparison dual injections of Fluoro-Gold and Fluoro-Ruby targeted at posterior VO or AI produced similar patterns of termination for

both the retrograde (FG) and anterograde tracer (FR). By plotting the mean location of labelling in temporal and sensory-motor cortex, some differences between dual and single injections can be seen. In temporal cortex, labelling from the dual injection into posterior VO (Bp) has a more lateral (i.e. superficial) mean location for anterograde labelling in temporal cortex than the equivalent single injection (Figure 10iii). In sensory-motor cortex, retrograde labelling from the dual injection into posterior VO (Bp) has a more ventral mean location (Figure 12i). The mean location of retrograde labels in sensory-motor cortex has a more lateral mean location resultant from the posterior VO dual injection (Bp), and for the posterior DLO (Dp) dual injection anterograde labelling has a more lateral mean location ((Figure 12iii). Although the mean location of labels show these minor differences between dual and single injections, the general pattern of connections remains consistent (figures 5 – 8). The results of these dual injections are shown in Figures 9-12 which are described below.

We plotted the location of the anterograde and retrograde tracer in three axes of orientation (dorsoventral, anterior-posterior and mediolateral) within both the temporal and sensory-motor cortex regions (see Figures 7-10). The graphs also include the data produced from dual injections targeted at anterior VO and DLO and posterior VO and AI. The location data within temporal cortex is shown following anterior (Figure 9) and posterior (Figure 10) PFC injections. The anterograde and retrograde labelling shows locational differences in temporal cortex for both anterior and posterior injections, however the clearest difference appears in the plotting along the anterior-posterior axis following anterior PFC injections (Figure 9ii): note the difference in retrograde and anterograde positions after injections denoted Ba and Da following single injections, in DLO this occurs following single or dual injections. By contrast the difference in anterograde and retrograde labelling following single injections into posterior PFC was much less marked in the anterior-posterior axis (Figure 10ii), this result was also observed following dual injections. The distribution of anterograde and retrograde tracer in the dorsoventral axis showed no obvious trends in terms of topology following anterior (Fig9i) or posterior (Fig 10i) PFC injections. The distribution within the mediolateral axis following

anterior injections also produced no clear arrangement for anterograde or retrograde tracer (Fig 9iii). However, the posterior PFC injections appear to produce a systematic shift between PFC injection sites (between MO and DLO): here we observed retrograde projections occurring at increasingly lateral locations within temporal cortex, i.e. superficially within cortex (Fig 10iii).

The location data within sensory-motor cortex following anterior and posterior PFC injections is shown in figures 11 and 12 respectively and the graphs include the data produced from dual injections. Again, the anterograde and retrograde labelling shows locational differences in sensory-motor cortex for both anterior and posterior injections, and like the temporal cortex results, note the difference in positions of anterograde efferents and retrograde afferents in the anterior-posterior axis following single anterior PFC injections (Figure 11ii – injections denoted Aa, Ba and Da). Dual injections also produced differences in the terminal locations for FG and FR. As was the case for the temporal cortex labelling, the difference in anterograde and retrograde labelling following injections into posterior PFC was less marked in the anterior-posterior axis (Figure 12ii) – this was observed following both single and dual injections. The distribution of anterograde efferents in the dorsoventral axis of sensory-motor cortex showed no obvious trends in terms of topology following anterior PFC injections (Fig11i), however the posterior single injections of FG tracer resulted in an apparent topological arrangement of retrograde terminals, with increasingly ventrally located cell bodies occurring between injection sites MO and AI (Fig 12i). The distribution within the mediolateral axis following anterior injections produced no clear arrangement for anterograde efferents or retrograde afferents following anterior (Fig 11iii) or posterior PFC injections (Fig 12iii).

Discussion

Our study is the first to provide detailed analysis of how the topology of connections changes within anterior and posterior portions of rat PFC. Further, we report that there are changes in the arrangement

of connections to both temporal and sensory motor cortices at anterior or posterior levels of rat prefrontal cortex.

Methodological and Interpretative Considerations

Our results have shown that the FG injections produced retrograde labelling and our FR injections primarily produced anterograde labelling. For FR labelling we base this judgement on the majority of labelling not co-localising with alpha-tubulin (a cytoplasmic marker). We used relatively large tracer injections (of 100nl FG and 100nl FR) because this produced a consistent and repeatable injection volume that ensured significant labelling within the projection sites (i.e. connected regions). We cannot rule out some spread to fibers of passage. The size of the tracer injections inevitably also meant that tracer was not usually confined to just one sub-region of PFC, in the case of PL injections there was also some spread into secondary motor cortex. In addition, our comparison of single injections revealed that these were not identical in terms of mean location of projection label (figures 9-12) however an analysis of their distributions showed a very similar overall distribution (figures 5-8). Here we aimed to look at how connectional architecture changes at anterior and posterior PFC levels, however the changing shape and architecture of PFC in the A-P axis provided limitations to the study (see below for a detailed discussion). It is worth also pointing out that our terms of ‘anterior’ and ‘posterior’ PFC are relative, as there are significant anterior and posterior regions beyond the levels we have studied (approximately 1mm anterior and approximately 2mm posterior). Therefore the levels of PFC studied in this paper should both be considered to be central regions.

Organisation of Connections from Anterior and Posterior Prefrontal Cortex to Temporal Cortex

In this study we observed apparent topology of connections in the location of anterograde and retrograde connections from both anterior and posterior PFC and to both temporal and sensory-motor cortex.

In addition we found that for *anterior PFC* this topology of connections differed for the anterograde and retrograde tracers employed. In other words, the distribution of retrograde and anterograde labelling occurred in different sub-regions of temporal cortex. The differences were most notable following injections into medial orbital cortex (i.e. VO) or following injections into DLO (i.e lateral PFC). This is of interest because it produced a very similar topology and distribution of afferents/efferents to that found following tracer injections into a ‘central’, coronal portion of PFC (Bedwell et al, 2015), located at the equivalent coronal level of bregma +4.2mm (a coronal level half way between the 2 sections in figure 1 of the present study). Specifically Fluoro-Gold and Fluoro-Ruby injections into VO, VLO and DLO at this level produced afferents or efferents in correspondingly similar positions within temporal and sensory-motor cortex. This study also found that the distribution of anterograde and retrograde axon terminals/projecting neurons did not correspond (particularly in the case of VO and DLO).

Further to this, we found that for the posterior PFC region we studied, the topology and distribution of Fluoro-Gold (retrograde) afferents and Fluoro-Ruby (anterograde) efferents were much more similar. In the case of posterior PFC; VO, MO, IL and PL (medial orbital) and LO, AI, DI and GI (lateral PFC) labelled retrograde cells and anterograde axon terminals occurred in relatively similar locations (in comparison to equivalent distributions following equivalent anterior medial orbital (VO) and lateral orbital (DLO) injections). There could be several possible reasons for this dissociation between anterior and posterior PFC. The first and most plausible reason is that the cytoarchitectural regions compared are not equivalent. The most lateral injections made into the anterior PFC occupied DLO, at the posterior PFC level studied the most lateral injection occupied predominantly agranular insular cortex. This may explain the disparity seen in terms of different locations of retrograde afferents (DLO versus AI). By examining the injection locations of the most medial orbital injections

(anterior versus posterior) it is also clear that, due to the changing shape of PFC subdivisions, tracer occupied different subdivisions (anterior PFC: predominantly VO and MO; posterior PFC: VO, MO, IL, PL). These cytoarchitectural differences in terms of injection site may help to explain the apparent differences, notably in relation to the distribution of retrograde tracer. Another possible interpretation for these differences is that there is a broad organisational difference within rat prefrontal cortex, where anterior and central regions of PFC contain many non-reciprocal connections and posterior PFC connections are more reciprocal in nature.

Organisation of Connections from Anterior and Posterior Prefrontal Cortex to the Sensory-Motor Cortex

We observed strong connections between prefrontal cortex and the sensory-motor cortex. A previous study has reported connections between rat orbital cortex and the cingulate cortex and secondary somatic sensory motor area (Reep et al., 1996). The rat precentral medial area is also known to connect to somatosensory cortex (Conde et al., 1995). In primates S1 receives afferent connections from premotor areas (Cerkevich et al., 2014). Projections from the sensory-motor cortex region to the different PFC regions frequently arose from distinct cortical layers within somatosensory cortex, this resembled a similar pattern of projections from the striatum to the medial PFC described previously (Gabbott et al., 2005) and was in agreement with our previous report concerning the connections of central PFC (Bedwell et al 2014). Within the two coronal levels studied here we saw a topology prominent within the connections to sensory-motor cortex of the orbital region of cortex. In common with the temporal cortex connections, the topology of sensory-motor cortex-PL connections did not fit within the arrangement of orbital connections (again for both FG and FR afferents/efferents). A similar pattern of labelling was observed in the PFC-sensory-motor connections as was seen in the PFC-temporal connections. Here the topology of anterograde and retrograde connections (arising from the orbital region) differed for equivalent injections in the anterior level. However at the posterior coronal level the topology observed was similar for retrograde afferents and anterograde efferents seen within temporal cortex. Similarly at the level of individual injection sites this meant

that for posterior PFC, VO, MO, IL and PL (medial orbital) and LO, AI, DI and GI (lateral PFC), labelling of retrograde afferents and anterograde efferents occurred in relatively similar locations (in comparison to equivalent distributions following equivalent anterior medial orbital (VO) and lateral orbital (DLO) injections). The reasons for this disparity are discussed in the preceding section on PFC-temporal cortex connections.

Our analysis also shows that, in general, the distributional spread of connections became more widespread in the target regions following more posteriorly located PFC injections (this was particularly clear in the spread of connections to sensory-motor cortex shown in figure 6). This was the case for both anterograde and retrograde connections. This indicates that there was a change in the organisational patterns of divergence and convergence as we move from anterior to posterior PFC. This additional change in the organisation of connections could have important implications for key processing characteristics within PFC circuits.

Conclusions

Clearly the organisation of cortical connections has important functional consequences in terms of both physiological organisation and function. The topology and topography of cortical connections to sensory cortices supports (1) the existence of both sensory and cognitive maps and (2) important perceptual functions such as visual feedback (Wang et al., 2006) and attention (Tootell et al., 1982). Our study is in agreement with and provides further evidence for topologically arranged projections arising from and projecting to rat PFC. Additionally our results provide evidence that the anterograde and retrograde connections to orbital PFC differ in terms of their relative position and that this varies according to the coronal level within PFC. In general we observed that our more posteriorly placed injections produced anterograde efferents and retrograde afferents in more similar cortical positions,

compared to the more anteriorly placed injections. It remains to be seen whether such a trend continues at progressively anterior and posterior positions within PFC. However the results indicate that there are changes in the relative degree of reciprocity of connections within different regions of PFC and this is likely to have important consequences for cortical processing in this important brain region.

Acknowledgements

This work was supported by a Nottingham Trent University studentship awarded to Stacey Bedwell. We would like to thank Andrew Marr and Danielle MacDonald for their technical support.

Data Statement

On acceptance of this article we plan to deposit the connectome data on the University of Rostock rat connectome website: <http://neuroviisas.med.uni-rostock.de/connectome/index.php>. The Data File(s) will also be deposited to Figshare.

References

- Agster KL, Burwell RD (2013) Hippocampal and subicular efferents and afferents of the perirhinal, postrhinal, and entorhinal cortices of the rat. *Behav Brain Res (Netherlands)* 254:50-64.
- Alvarez JA, Emory E (2006) Executive function and the frontal lobes: A meta-analytic review. *Neuropsychol Rev (United States)* 16:17-42.
- Arnault P, Roger M (1990) Ventral temporal cortex in the rat: Connections of secondary auditory areas Te2 and Te3. *J Comp Neurol (UNITED STATES)* 302:110-123.
- Aronoff R, Matyas F, Mateo C, Ciron C, Schneider B, Petersen CC (2010) Long-range connectivity of mouse primary somatosensory barrel cortex. *Eur J Neurosci (France)* 31:2221-2233.
- Bedwell SA, Billett EE, Crofts JJ, Tinsley CJ (2014) The topology of connections between rat prefrontal, motor and sensory cortices. *Front Syst Neurosci (Switzerland)* 8:177.
- Bedwell SA, Billett EE, Crofts JJ, MacDonald DM, Tinsley CJ (2015) The topology of connections between rat prefrontal and temporal cortices. *Front Syst Neurosci (Switzerland)* 9:80.
- Berendse HW, Galis-de Graaf Y, Groenewegen HJ (1992) Topographical organization and relationship with ventral striatal compartments of prefrontal corticostriatal projections in the rat. *J Comp Neurol (UNITED STATES)* 316:314-347.
- Burwell RD, Witter MP, Amaral DG (1995) Perirhinal and postrhinal cortices of the rat: A review of the neuroanatomical literature and comparison with findings from the monkey brain. *Hippocampus (UNITED STATES)* 5:390-408.
- Cerkevich CM, Qi HX, Kaas JH (2014) Corticocortical projections to representations of the teeth, tongue, and face in somatosensory area 3b of macaques. *J Comp Neurol (United States)* 522:546-572.

Conde F, Maire-Lepoivre E, Audinat E, Crepel F (1995) Afferent connections of the medial frontal cortex of the rat. II. cortical and subcortical afferents. *J Comp Neurol (UNITED STATES)* 352:567-593.

Delatour B, Witter MP (2002) Projections from the parahippocampal region to the prefrontal cortex in the rat: Evidence of multiple pathways. *Eur J Neurosci (France)* 15:1400-1407.

Fryszak RJ, Neafsey EJ (1994) The effect of medial frontal cortex lesions on cardiovascular conditioned emotional responses in the rat. *Brain Res (NETHERLANDS)* 643:181-193.

Fuster JM (2001) The prefrontal cortex--an update: Time is of the essence. *Neuron (United States)* 30:319-333.

Gabbott PL, Warner TA, Jays PR, Salway P, Busby SJ (2005) Prefrontal cortex in the rat: Projections to subcortical autonomic, motor, and limbic centers. *J Comp Neurol (United States)* 492:145-177.

Gattass R, Nascimento-Silva S, Soares JG, Lima B, Jansen AK, Diogo AC, Farias MF, Botelho MM, Mariani OS, Azzi J, Fiorani M (2005) Cortical visual areas in monkeys: Location, topography, connections, columns, plasticity and cortical dynamics. *Philosophical Transactions of the Royal Society of London* 360:709-31.

Goulden N, McKie S, Thomas EJ, Downey D, Juhasz G, Williams SR, Rowe JB, Deakin JF, Anderson IM, Elliott R (2012) Reversed frontotemporal connectivity during emotional face processing in remitted depression. *Biol Psychiatry (United States)* 72:604-611.

Henry EC, Catania KC (2006) Cortical, callosal, and thalamic connections from primary somatosensory cortex in the naked mole-rat (*heterocephalus glaber*), with special emphasis on the connectivity of the incisor representation. *Anat Rec A Discov Mol Cell Evol Biol (United States)* 288:626-645.

Hoover WB, Vertes RP (2011) Projections of the medial orbital and ventral orbital cortex in the rat. *J Comp Neurol (United States)* 519:3766-3801.

Kim J, Ghim JW, Lee JH, Jung MW (2013) Neural correlates of interval timing in rodent prefrontal cortex. *J Neurosci (United States)* 33:13834-13847.

Kolb B (1984) Functions of the frontal cortex of the rat: A comparative review. *Brain Res (NETHERLANDS)* 320:65-98.

Kondo H, Witter MP (2014) Topographic organization of orbitofrontal projections to the parahippocampal region in rats. *J Comp Neurol (United States)* 522:772-793.

Krettek JE, Price JL (1977) The cortical projections of the mediodorsal nucleus and adjacent thalamic nuclei in the rat. *J Comp Neurol (UNITED STATES)* 171:157-191.

Narayanan NS, Laubach M (2009) Delay activity in rodent frontal cortex during a simple reaction time task. *J Neurophysiol (United States)* 101:2859-2871.

Narayanan NS, Laubach M (2008) Neuronal correlates of post-error slowing in the rat dorsomedial prefrontal cortex. *J Neurophysiol (United States)* 100:520-525.

Narayanan NS, Laubach M (2006) Top-down control of motor cortex ensembles by dorsomedial prefrontal cortex. *Neuron (United States)* 52:921-931.

Neafsey EJ (1990) Prefrontal cortical control of the autonomic nervous system: Anatomical and physiological observations. *Prog Brain Res (NETHERLANDS)* 85:147-65; discussion 165-6.

Olson CR, Musil SY (1992) Topographic organization of cortical and subcortical projections to posterior cingulate cortex in the cat: Evidence for somatic, ocular, and complex subregions. *The Journal of Comparative Neurology* 324:237-60.

Paxinos G, Watson C (1998) The rat brain in stereotaxic coordinates. San Diego, CA: Academic Press.

Porter LL, White EL (1983) Afferent and efferent pathways of the vibrissal region of primary motor cortex in the mouse. *J Comp Neurol (UNITED STATES)* 214:279-289.

Reep RL, Corwin JV, King V (1996) Neuronal connections of orbital cortex in rats: Topography of cortical and thalamic afferents. *Exp Brain Res (GERMANY)* 111:215-232.

Schilman EA, Uylings HB, Galis-de Graaf Y, Joel D, Groenewegen HJ (2008) The orbital cortex in rats topographically projects to central parts of the caudate-putamen complex. *Neurosci Lett (Ireland)* 432:40-45.

Schoenbaum G, Esber GR (2010) How do you (estimate you will) like them apples? integration as a defining trait of orbitofrontal function. *Curr Opin Neurobiol (England)* 20:205-211.

Schoenbaum G, Roesch M (2005) Orbitofrontal cortex, associative learning, and expectancies. *Neuron (United States)* 47:633-636.

Sesack SR, Deutch AY, Roth RH, Bunney BS (1989) Topographical organization of the efferent projections of the medial prefrontal cortex in the rat: An anterograde tract-tracing study with phaseolus vulgaris leucoagglutinin. *J Comp Neurol (UNITED STATES)* 290:213-242.

Smith NJ, Horst NK, Liu B, Caetano MS, Laubach M (2010) Reversible inactivation of rat premotor cortex impairs temporal preparation, but not inhibitory control, during simple reaction-time performance. *Front Integr Neurosci (Switzerland)* 4:124.

Stalnaker TA, Cooch NK, Schoenbaum G (2015) What the orbitofrontal cortex does not do. *Nat Neurosci (United States)* 18:620-627.

Taren AA, Venkatraman V, Huettel SA (2011) A parallel functional topography between medial and lateral prefrontal cortex: Evidence and implications for cognitive control. *J Neurosci* (United States) 31:5026-5031.

Tootell RB, Silverman MS, Switkes E, De Valois RL (1982) Deoxyglucose analysis of retinotopic organization in primate striate cortex. *Science* (UNITED STATES) 218:902-904.

Van De Werd HJ, Uylings HB (2008) The rat orbital and agranular insular prefrontal cortical areas: A cytoarchitectonic and chemoarchitectonic study. *Brain Struct Funct* (Germany) 212:387-401.

Vertes RP (2006) Interactions among the medial prefrontal cortex, hippocampus and midline thalamus in emotional and cognitive processing in the rat. *Neuroscience* (United States) 142:1-20.

Vertes RP (2004) Differential projections of the infralimbic and prelimbic cortex in the rat. *Synapse* (United States) 51:32-58.

Wang W, Jones HE, Andolina IM, Salt TE, Sillito AM (2006) Functional alignment of feedback effects from visual cortex to thalamus. *Nat Neurosci* (United States) 9:1330-1336.

Rat ID	Hemisphere (L/R)	Tracer	AP	ML	Depth from cortical surface
11	Left	Fluoro-Gold	3.2	2.2	3.2
17	Left	Fluoro-Gold	4.2	2.2	3.2
21	Right	Fluoro-Ruby	4.2	2.2	3.2
22	Left	Fluoro-Gold	3.2	1.2	3.2
23	Right	Fluoro-Ruby	4.2	1.2	3.2
23	Left	Fluoro-Gold	4.2	3.2	3.2
24	Right	Fluoro-Ruby	4.2	3.2	3.2
24	Left	Fluoro-Gold	4.2	1.2	3.2
25	Right	Fluoro-Ruby	3.2	2.2	3.2
26	Left	Fluoro-Gold	3.2	3.2	3.2
26	Right	Fluoro-Ruby	3.2	1.2	3.2
27	Right	Fluoro-Ruby	3.2	3.2	3.2
27	Left	Fluoro-Gold	3.2	1.2	2.4
28	Left	Fluoro-Gold	4.2	1.2	2.4
28	Right	Fluoro-Ruby	3.2	1.2	2.4
32	Right	Fluoro-Ruby	4.2	1.2	2.4
37	Right	Fluoro-Ruby	4.2	2.2	1.0
38	Right	Fluoro-Ruby	4.2	3.2	1.0
39	Left	Fluoro-Ruby	3.7	1.2	3.2
55	Left	Fluoro-Ruby & Fluoro-Gold	3.2	1.2	3.2
56	Left	Fluoro-Ruby & Fluoro-Gold	3.2	3.2	3.2
57	Left	Fluoro-Ruby & Fluoro-Gold	4.2	1.2	3.2
58	Left	Fluoro-Ruby & Fluoro-Gold	4.2	3.2	3.2

Table 1. Stereotaxic location of tracer injections for each individual rat (i.e. intended locations). Stereotaxic location in terms of anterior-posterior (AP) distance with respect to bregma (these reflect the surgical stereotaxic coordinates rather than the histological coordinates confirmed later, which were slightly anterior), medial lateral (ML) distance with respect to bregma and **depth from cortical surface** (all in mm). The tracer type and hemisphere is also provided.

Figure Legends

Figure 1. Tracer injections into posterior and anterior prefrontal regions. (i) Coronal section of anterior PFC (+4.7mm anterior to Bregma) showing the cytoarchitectural boundaries of PFC sub-regions according to Van de Werd & Uylings (2008), depicting sites of tracer injections; PL (Aa), VO (Ba), VLO (Ca) and DLO (Da), with 1mm separation. (ii) Representations of Fluoro-Ruby (100nl) (R21, R23, R24, R32 (broken line)) injection sites in anterior PL and FrA (R32), VO and MO (R23), VLO and FrA (R21) and DLO (R24) in the right hemisphere. Representations of Fluoro-Gold (100nl) (R17, R23, R24, R28 (solid line)) and dual Fluoro-Gold (100nl) and Fluoro-Ruby (100nl) (R57, R58 (broken grey line)) injection sites in anterior PL, MO and VO (R28), VO and MO (R24, R57), VLO (R17) and DLO and LO (R23, R58) in the left hemisphere. (iii) Coronal section of posterior PFC (+3.7mm anterior to Bregma) showing the cytoarchitectural boundaries of PFC sub-regions according to Van de Werd & Uylings (2008), depicting intended sites of tracer injections; PL (Ap), VO (Bp), VLO (Cp) and AI (Dp), with 1mm separation. (iv) Representations of Fluoro-Ruby (100nl) (R25, R26, R27, R28 (broken line)) injection sites in PL, Cg1 and M2 (R28), VO, MO, PL and IL (R26), VLO (R25) and AI, LO, DI and GI (R27), in the right hemisphere. Representations of Fluoro-Gold (100nl) (R11, R22, R26, R27 (solid line)) and dual Fluoro-Ruby (100nl) and Fluoro-Gold (100nl) (R55, R56 (broken grey line)) injection sites in PL, Cg1 and M2 (R27), VO, MO, PL and IL (R22, R55), VLO and M2 (R11) and LO, AI, DI and GI (R26, R56), in the left hemisphere. The diagrams represent an amalgamation of injection sites from the animals indicated by the 'R' number.

Figure 2. Coronal sections showing retrogradely labelled cells (blue) in temporal cortex produced by injections of 100nl Fluoro-Gold into (i) anterior VO (R24), (ii) posterior VO (R22) (x4) and (iii) high magnification photomicrograph showing posterior PL (R27) (x20). Propidium Iodide was used to stain the background cells (red). Coronal sections showing anterograde labelling (red) in temporal cortex produced by 100nl Fluoro-Ruby injections into (iv) anterior VO (R23), (v) posterior VO (R26) (x4) and (vi) high magnification photomicrograph showing Fluoro-Ruby labelling from injection into posterior VLO (R25) (x20). DAPI was used to stain the background cells (blue). The triangles denote the location of the rhinal sulcus. Arrows indicate locations of Fluoro-Ruby labelling. Scale bars = 100µm.

Figure 3. Coronal sections showing retrogradely labelled cells (blue) in sensory-motor cortex produced by injections of 100nl Fluoro-Gold into (i) anterior VO (R24), (ii) posterior VO (R22) (x4) and (iii) high magnification photomicrograph showing anterior VO (R24) (x20). Propidium Iodide was used to stain the background cells (red). Coronal sections showing anterograde labelling (red) in temporal cortex produced by 100nl Fluoro-Ruby injections into (iv) anterior VO (R23) (x4), (v) posterior VO (R26) (x4) and (vi) high magnification photomicrograph showing posterior VO (R26) (x20). DAPI was used to stain the background cells (blue). Scale bars = 100µm.

Figure 4. (i, ii & iii) Images of temporal cortex depicting fluorescently (fluorescein) labelled alpha tubulin (green) and Fluoro-Ruby labelling (red) resultant from (100nl) injection into PFC (Animal ID = R39). (iv) Image of temporal cortex depicting fluorescently labelled alpha tubulin (green), DAPI labelled nuclei (blue) and Fluoro-Ruby labelling (red) resultant from (100nl) injection into PFC. Dual-labelling of Fluoro-Ruby and Fluorescein (alpha tubulin) is shown by yellow fluorescence (iii). Scale bars = 20µm.

Figure 5. Diagram representing both retrograde (Fluoro-Gold) and anterograde (Fluoro-Ruby) projections to temporal cortex arising from tracer injections into the anterior and posterior PFC. (i) retrograde labelling in temporal cortex produced by Fluoro-Gold (100nl) injections into anterior PFC and (ii) posterior PFC. (iii) anterograde labelling in temporal cortex produced by Fluoro-Ruby

(100nl) injections into anterior PFC and (iv) posterior PFC. The diagrams represent an amalgamation of injection sites from the animals included in the study.

Figure 6. Diagram representing both retrograde (Fluoro-Gold) and anterograde (Fluoro-Ruby) projections to sensory-motor cortex arising from tracer injections into the anterior and posterior PFC. (i) retrograde labelling in sensory-motor produced by Fluoro-Gold (100nl) injections into anterior PFC and (ii) posterior PFC. (iii) anterograde labelling in sensory-motor cortex produced by Fluoro-Ruby (100nl) injections into anterior PFC and (iv) posterior PFC. The diagrams represent an amalgamation of injection sites from the animals included in the study.

Figure 7. Diagram representing both retrograde (Fluoro-Gold) and anterograde (Fluoro-Ruby) projections to temporal cortex arising from dual tracer injections into anterior and posterior PFC. (i) retrograde labelling in temporal cortex produced by Fluoro-Gold, from dual injections into anterior PFC and (ii) posterior PFC. (iii) anterograde labelling in temporal cortex produced by Fluoro-Ruby, from dual injections into anterior PFC and (iv) posterior PFC.

Figure 8. Diagram representing both retrograde (Fluoro-Gold) and anterograde (Fluoro-Ruby) projections to sensory-motor cortex arising from dual tracer injections into anterior and posterior PFC. (i) retrograde labelling in sensory-motor produced by Fluoro-Gold, from dual injections into anterior PFC and (ii) posterior PFC. (iii) anterograde labelling in sensory-motor cortex produced by Fluoro-Ruby, from dual injections into anterior PFC and (iv) posterior PFC.

Figure 9. The mean effect of anterior PFC injection site on the location of retrograde (Aa n=75, Ba n=102 [dual injection n=157], Ca n=334, Da n=67 [dual injection n=16]) and anterograde (Aa n=47, Ba n=29 [dual injection n=224], Ca n=113, Da n=31 [dual injection n=28]) afferents and efferents in temporal cortex in (i) dorsoventral, (ii) anterior-posterior and (iii) mediolateral axes. (iv) Coronal cross section of PFC indicating the position of four injection sites within PFC: Prelimbic (injection Aa), Ventral Orbital (injection Ba), Ventrolateral Orbital (injection Ca) and Dorsal Lateral Orbital (injection Da), coronal cross section of temporal cortex, depicting the three dimensions in which the locations of labelled cells were recorded. Error bars = standard error.

Figure 10. The mean effect of posterior PFC injection site on the location of retrograde (Ap n=114, Bp n=25 [dual injection n=159], Cp n=85, Dp n=45 [dual injection n=143]) and anterograde (Ap n=51, Bp n=36 [dual injection n=46], Cp n=113, Dp n=61 [dual injection n=213]) afferents and efferents in temporal cortex in (i) dorsoventral, (ii) anterior-posterior and (iii) mediolateral axes. (iv) Coronal cross section of PFC indicating the position of four injection sites within PFC: : PL,Cg1, M2 (injection Ap), VO,MO,IL,PL (injection Bp), VLO,M2 (injection Cp) [VLO alone in the case of the anterograde single injection] and LO,AI,DI,GI (injection Dp), coronal cross section of temporal cortex, depicting the three dimensions in which the locations of labelled cells were recorded. Error bars = standard error.

Figure 11. The mean effect of anterior PFC injection site on the location of retrograde (Aa n=20, Ba n=77 [dual injection n=313], Ca n=39, Da n=72 [dual injection n=134]) and anterograde (Aa n=87, Ba n=91 [dual injection n=322], Ca n=30, Da n=36 [dual injection n=45]) afferents and efferents in sensory-motor cortex in (i) dorsoventral, (ii) anterior-posterior and (iii) mediolateral axes. (iv) Coronal cross section of PFC indicating the position of four injection sites within PFC: Prelimbic (injection Aa), Ventral Orbital (injection Ba), Ventrolateral Orbital (injection Ca) and Dorsal Lateral Orbital (injection Da), coronal cross section of sensory-motor cortex, depicting the three dimensions in which the locations of labelled cells were recorded. Error bars = standard error.

Figure 12. The mean effect of posterior PFC injection site on the location of retrograde (Ap n=152, Bp n=268 [dual injection n=168], Cp n=136, Dp n=30 [dual injection n=227]) and anterograde (Ap n=124, Bp n=44 [dual injection n=41], Cp n=35, Dp n=40 [dual injection n=29]) afferents and efferents in sensory-motor cortex in (i) dorsoventral, (ii) anterior-posterior and (iii) mediolateral axes. (iv) Coronal cross section of PFC indicating the position of four injection sites within PFC: PL,Cg1, M2 (injection Ap), VO,MO,IL,PL (injection Bp), VLO,M2 (injection Cp) [VLO alone in the case of the anterograde single injection] and LO,AI,DI,GI (injection Dp), coronal cross section of sensory-motor cortex, depicting the three dimensions in which the locations of labelled cells were recorded. Error bars = standard error.

Table 1. Stereotaxic location of tracer injections for each individual rat (i.e. intended locations). Stereotaxic location in terms of anterior-posterior (AP) distance with respect to bregma (these reflect the surgical stereotaxic coordinates rather than the histological coordinates confirmed later, which were slightly anterior), medial lateral (ML) distance with respect to bregma and depth from cortical surface (all in mm). The tracer type and hemisphere is also provided.

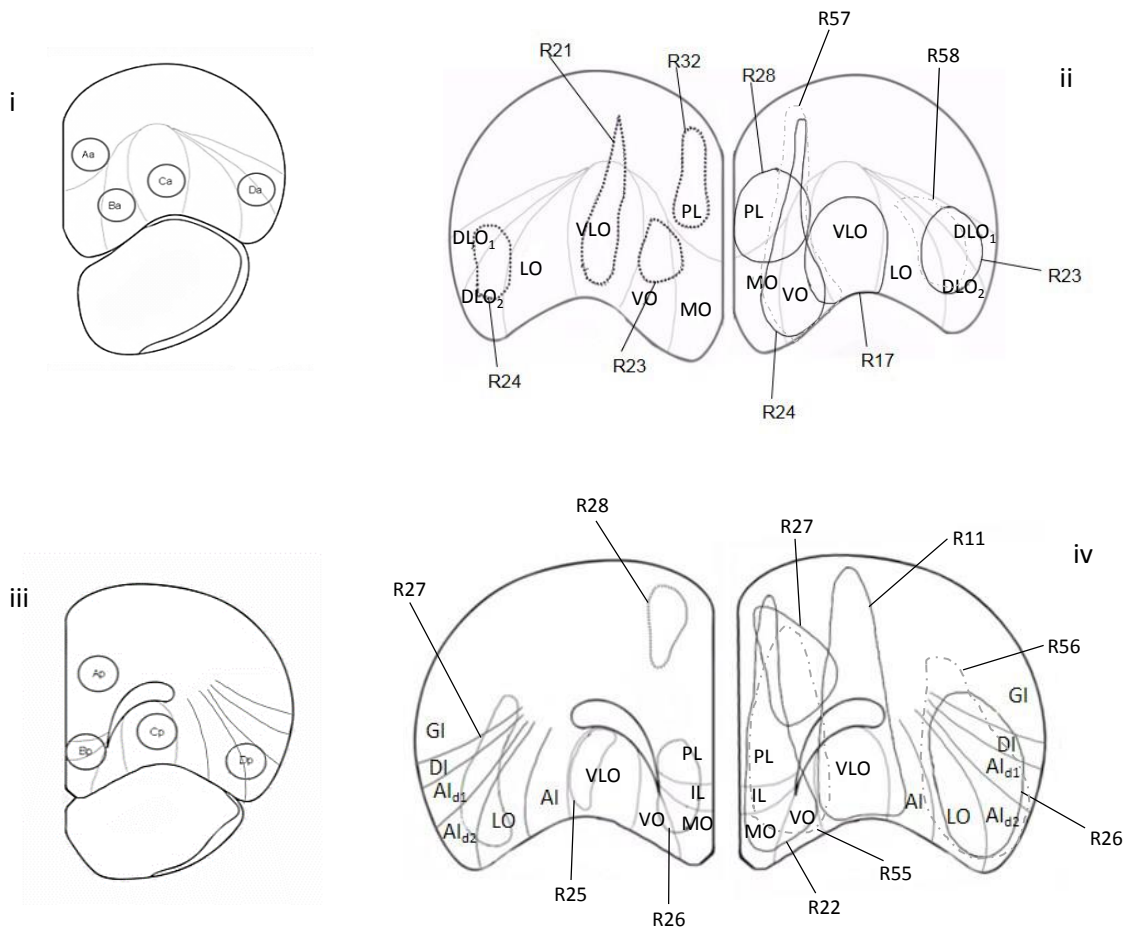


Figure 1. Tracer injections into posterior and anterior prefrontal regions. **(i)** Coronal section of anterior PFC (+4.7mm anterior to Bregma) showing the cytoarchitectural boundaries of PFC sub-regions according to Van de Werd & Uylings (2008), depicting sites of tracer injections; PL (Aa), VO (Ba), VLO (Ca) and DLO (Da), with 1mm separation. **(ii)** Representations of Fluoro-Ruby (100nl) (R21, R23, R24, R32 (broken line)) injection sites in anterior PL and FrA (R32), VO and MO (R23), VLO and FrA (R21) and DLO (R24) in the right hemisphere. Representations of Fluoro-Gold (100nl) (R17, R23, R24, R28 (solid line)) and dual Fluoro-Gold (100nl) and Fluoro-Ruby (100nl) (R57, R58 (broken grey line)) injection sites in anterior PL, MO and VO (R28), VO and MO (R24, R57), VLO (R17) and DLO and LO (R23, R58) in the left hemisphere. **(iii)** Coronal section of posterior PFC (+3.7mm anterior to Bregma) showing the cytoarchitectural boundaries of PFC sub-regions according to Van de Werd & Uylings (2008), depicting intended sites of tracer injections; PL (Ap), VO (Bp), VLO (Cp) and AI (Dp), with 1mm separation. **(iv)** Representations of Fluoro-Ruby (100nl) (R25, R26, R27, R28 (broken line)) injection sites in PL, Cg1 and M2 (R28), VO, MO, PL and IL (R26), VLO (R25) and AI, LO, DI and GI (R27), in the right hemisphere. Representations of Fluoro-Gold (100nl) (R11, R22, R26, R27 (solid line)) and dual Fluoro-Ruby (100nl) and Fluoro-Gold (100nl) (R55, R56 (broken grey line)) injection sites in PL, Cg1 and M2 (R27), VO, MO, PL and IL (R22, R55), VLO and M2 (R11) and LO, AI, DI and GI (R26, R56), in the left hemisphere. The diagrams represent an amalgamation of injection sites from the animals indicated by the 'R' number.

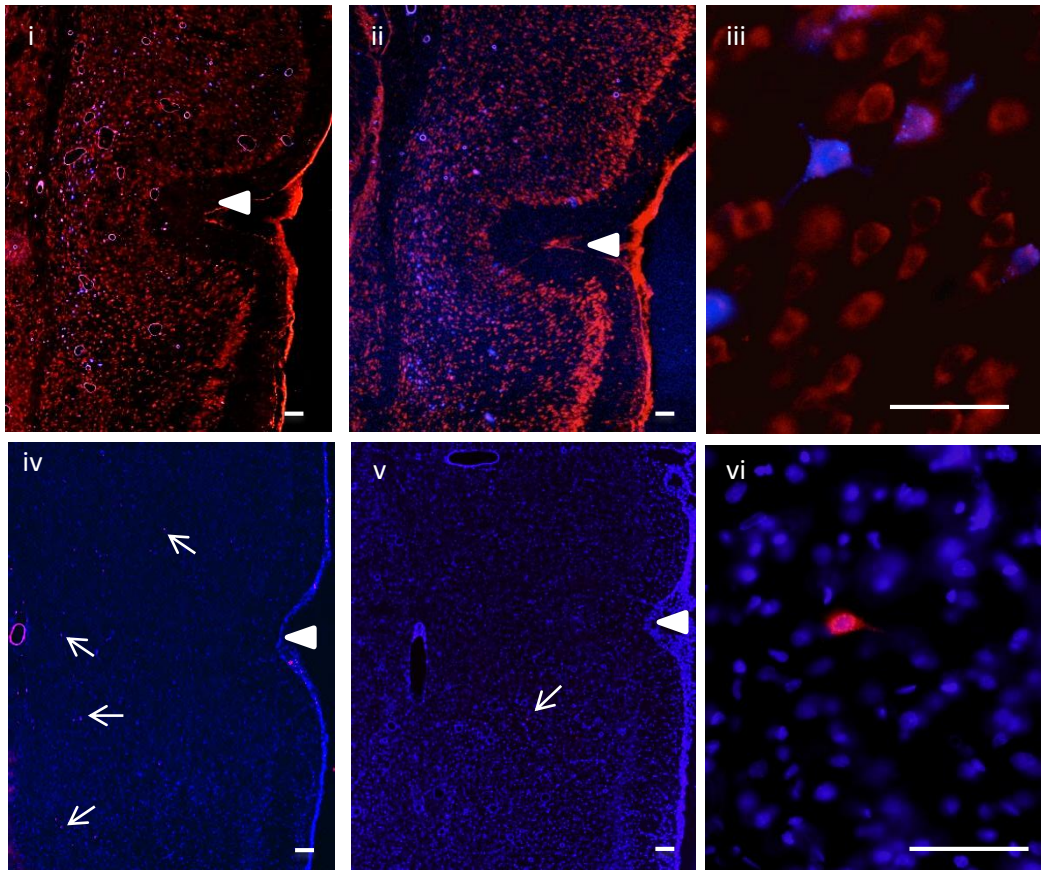


Figure 2. Coronal sections showing retrogradely labelled cells (blue) in temporal cortex produced by injections of 100nl Fluoro-Gold into **(i)** anterior VO (R24), **(ii)** posterior VO (R22) (x4) and **(iii)** high magnification photomicrograph showing posterior PL (R27) (x20). Propidium Iodide was used to stain the background cells (red). Coronal sections showing anterograde labelling (red) in temporal cortex produced by 100nl Fluoro-Ruby injections into **(iv)** anterior VO (R23), **(v)** posterior VO (R26) (x4) and **(vi)** high magnification photomicrograph showing Fluoro-Ruby labelling from injection into posterior VLO (R25) (x20). DAPI was used to stain the background cells (blue). The triangles denote the location of the rhinal sulcus. Arrows indicate locations of Fluoro-Ruby labelling. Scale bars = 100 μ m.

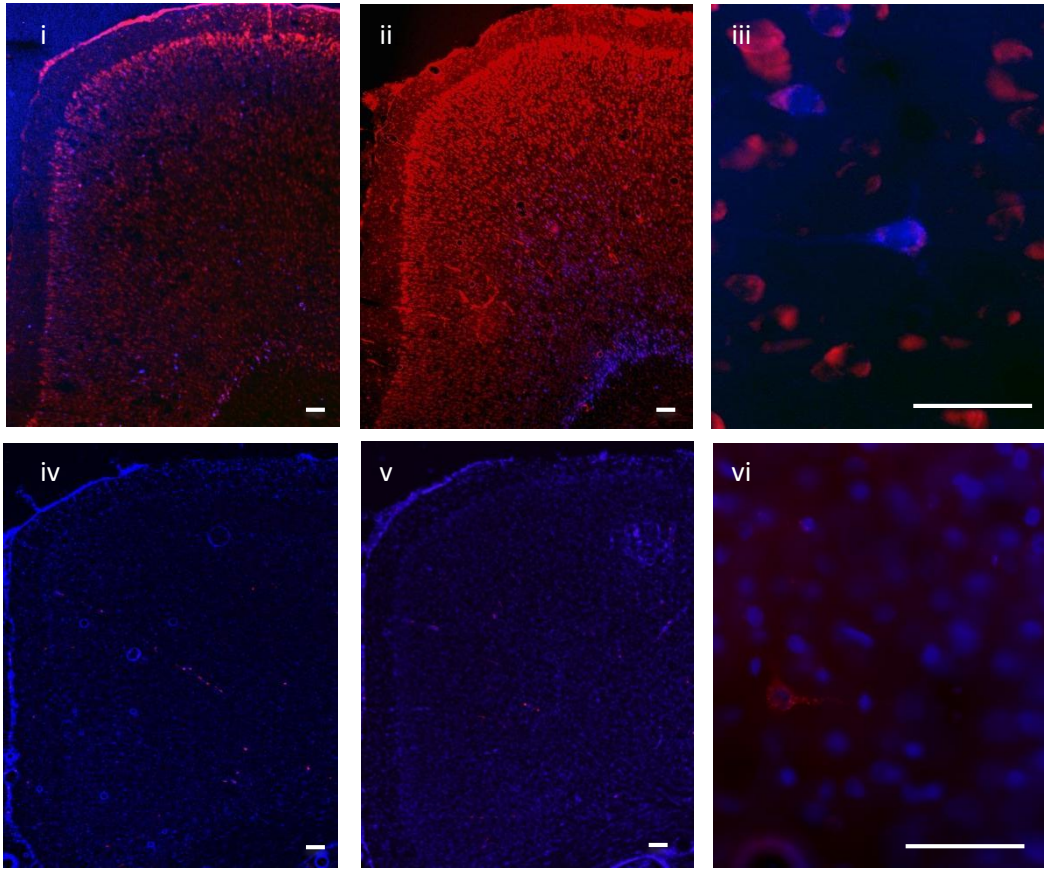


Figure 3. Coronal sections showing retrogradely labelled cells (blue) in sensory-motor cortex produced by injections of 100nl Fluoro-Gold into **(i)** anterior VO (R24), **(ii)** posterior VO (R22) (x4) and **(iii)** high magnification photomicrograph showing anterior VO (R24) (x20). Propidium Iodide was used to stain the background cells (red). Coronal sections showing anterograde labelling (red) in temporal cortex produced by 100nl Fluoro-Ruby injections into **(iv)** anterior VO (R23) (x4), **(v)** posterior VO (R26) (x4) and **(vi)** high magnification photomicrograph showing posterior VO (R26) (x20). DAPI was used to stain the background cells (blue). Scale bars = 100µm.

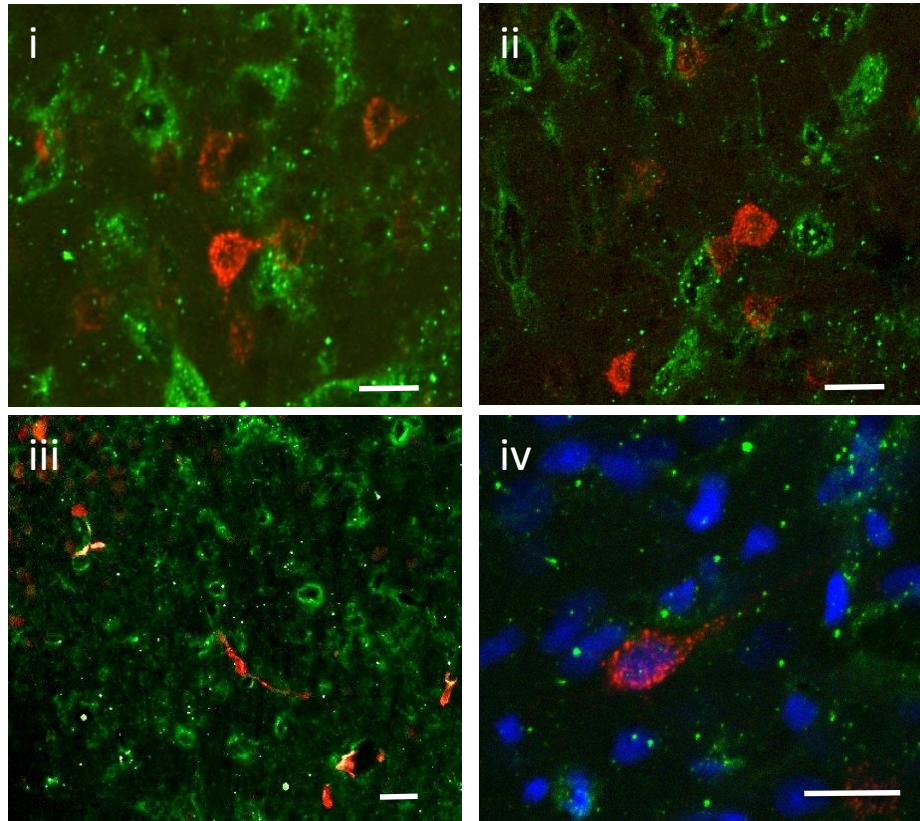


Figure 4. (i, ii & iii) Images of temporal cortex depicting fluorescently (fluorescein) labelled alpha tubulin (green) and Fluoro-Ruby labelling (red) resultant from (100nl) injection into PFC (Animal ID = R39). (iv) Image of temporal cortex depicting fluorescently labelled alpha tubulin (green), DAPI labelled nuclei (blue) and Fluoro-Ruby labelling (red) resultant from (100nl) injection into PFC. Dual-labelling of Fluoro-Ruby and Fluorescein (alpha tubulin) is shown by yellow fluorescence (iii). Scale bars = 20 μ m.

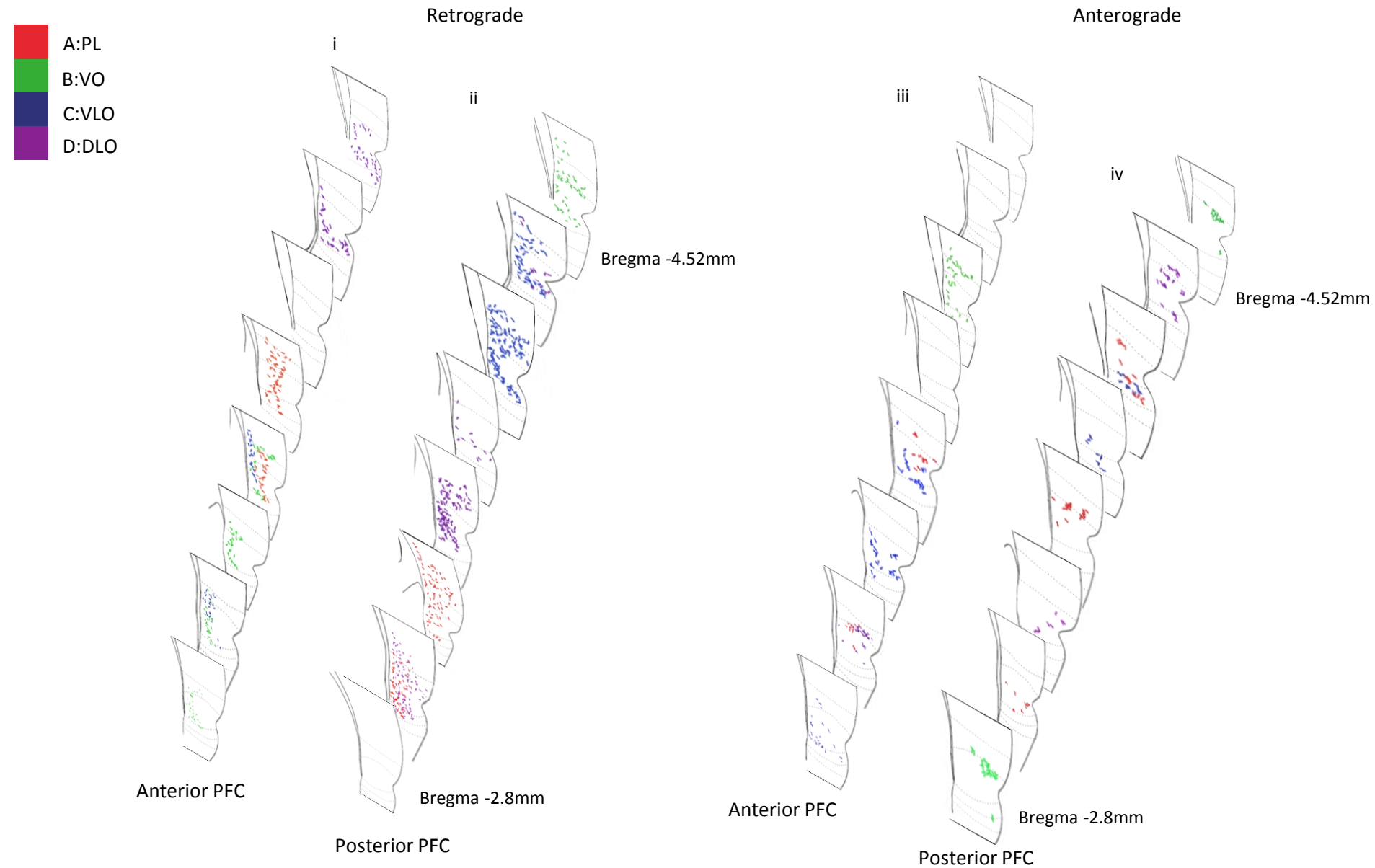


Figure 5. Diagram representing both retrograde (Fluoro-Gold) and anterograde (Fluoro-Ruby) projections to temporal cortex arising from tracer injections into the anterior and posterior PFC. **(i)** retrograde labelling in temporal cortex produced by Fluoro-Gold (100nl) injections into anterior PFC and **(ii)** posterior PFC. **(iii)** anterograde labelling in temporal cortex produced by Fluoro-Ruby (100nl) injections into anterior PFC and **(iv)** posterior PFC. The diagrams represent an amalgamation of injection sites from the animals included in the study.

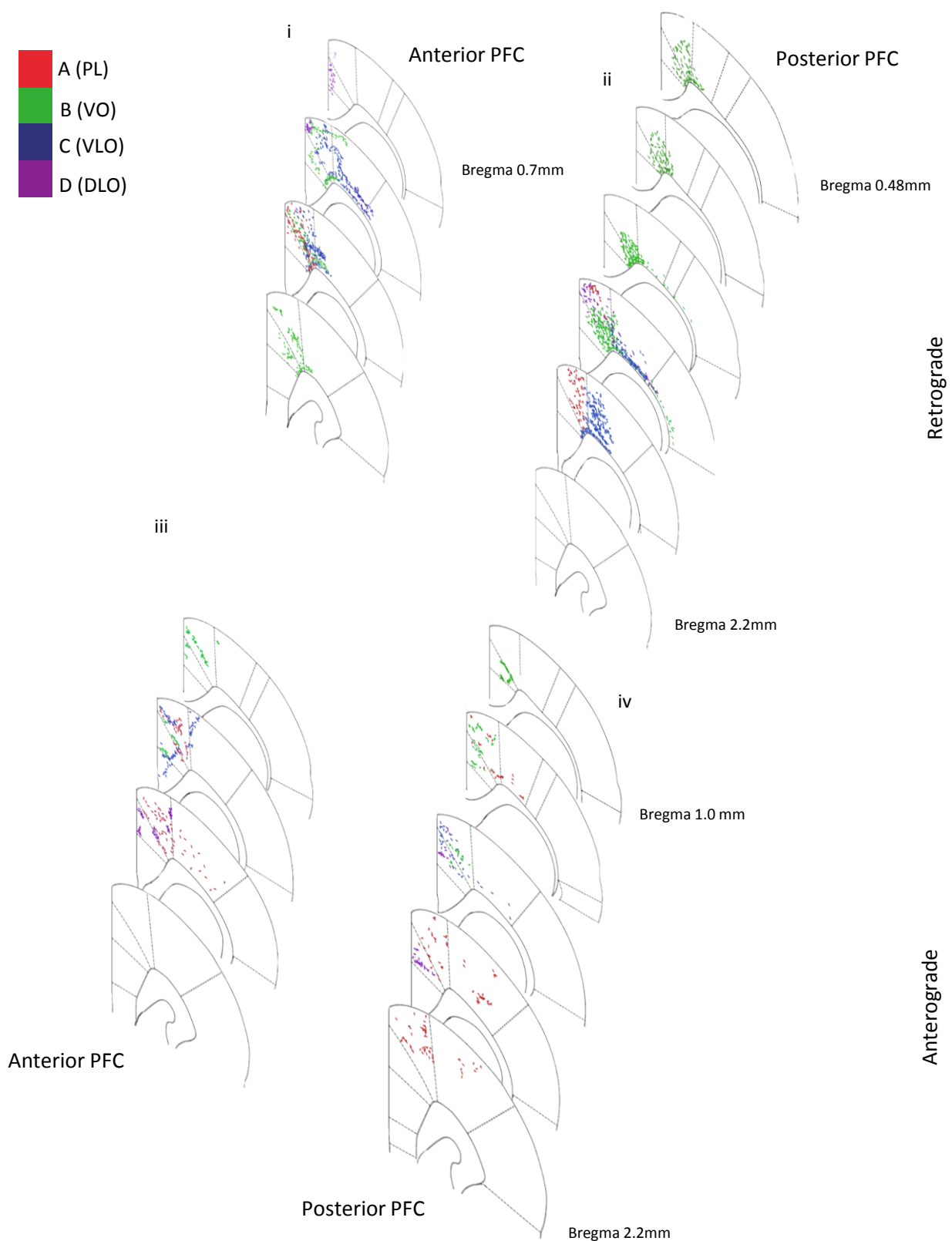


Figure 6. Diagram representing both retrograde (Fluoro-Gold) and anterograde (Fluoro-Ruby) projections to sensory-motor cortex arising from tracer injections into the anterior and posterior PFC. **(i)** retrograde labelling in sensory-motor produced by Fluoro-Gold (100nl) injections into anterior PFC and **(ii)** posterior PFC. **(iii)** anterograde labelling in sensory-motor cortex produced by Fluoro-Ruby (100nl) injections into anterior PFC and **(iv)** posterior PFC. The diagrams represent an amalgamation of injection sites from the animals included in the study.

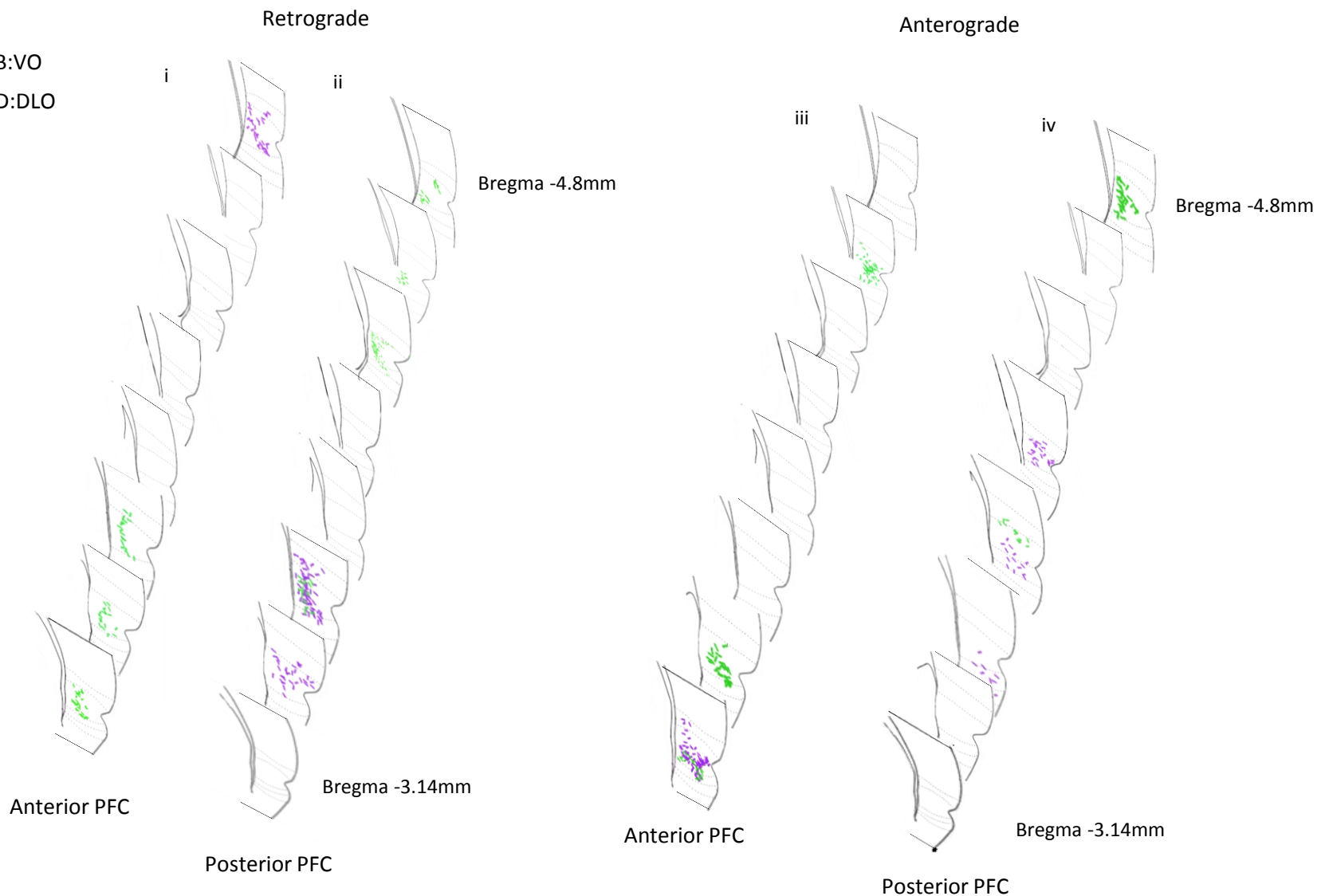


Figure 7. Diagram representing both retrograde (Fluoro-Gold) and anterograde (Fluoro-Ruby) projections to temporal cortex arising from dual tracer injections into anterior and posterior PFC. **(i)** retrograde labelling in temporal cortex produced by Fluoro-Gold, from dual injections into anterior PFC and **(ii)** posterior PFC. **(iii)** anterograde labelling in temporal cortex produced by Fluoro-Ruby, from dual injections into anterior PFC and **(iv)** posterior PFC.

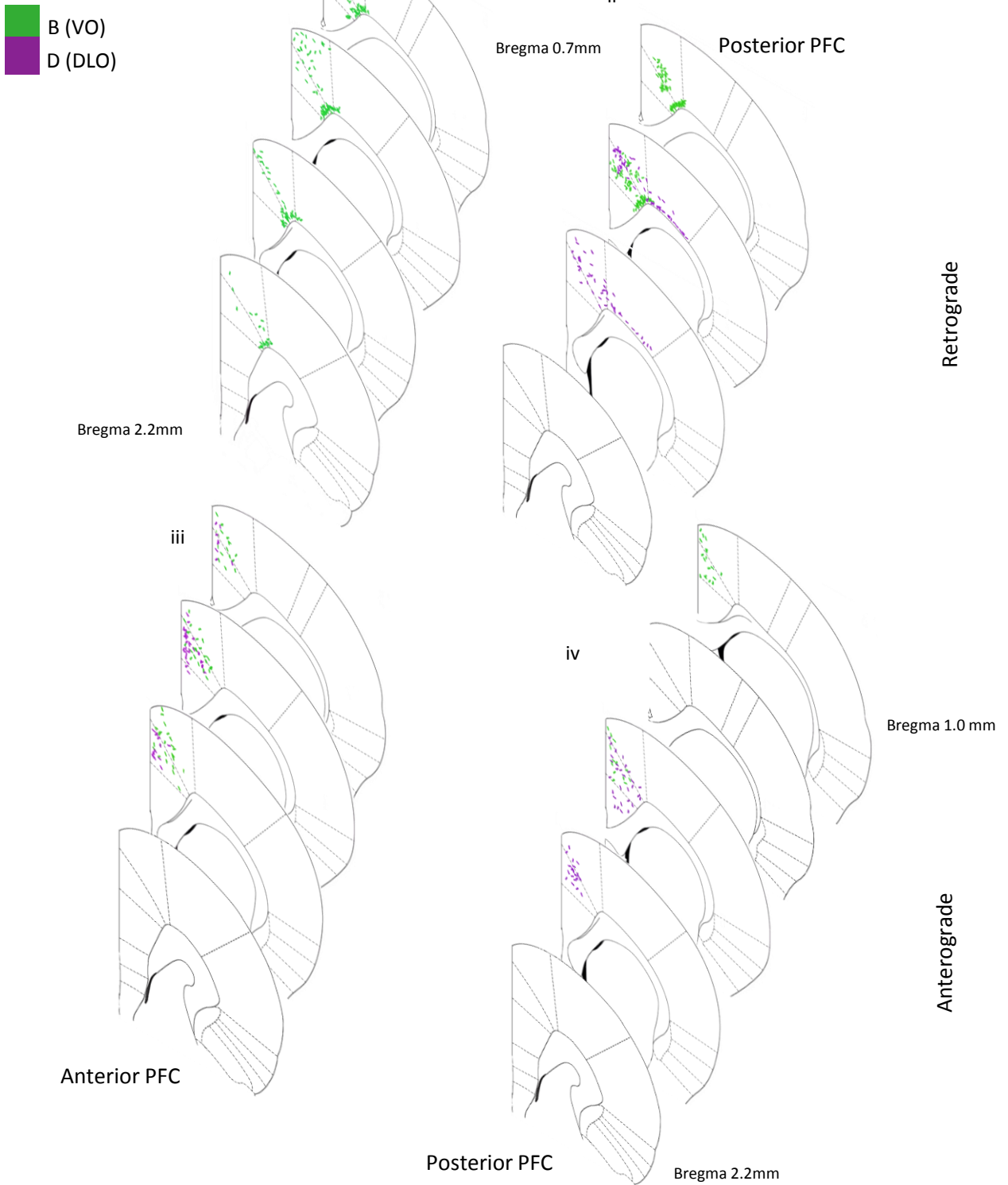


Figure 8. Diagram representing both retrograde (Fluoro-Gold) and anterograde (Fluoro-Ruby) projections to sensory-motor cortex arising from dual tracer injections into anterior and posterior PFC. **(i)** retrograde labelling in sensory-motor produced by Fluoro-Gold, from dual injections into anterior PFC and **(ii)** posterior PFC. **(iii)** anterograde labelling in sensory-motor cortex produced by Fluoro-Ruby, from dual injections into anterior PFC and **(iv)** posterior PFC.

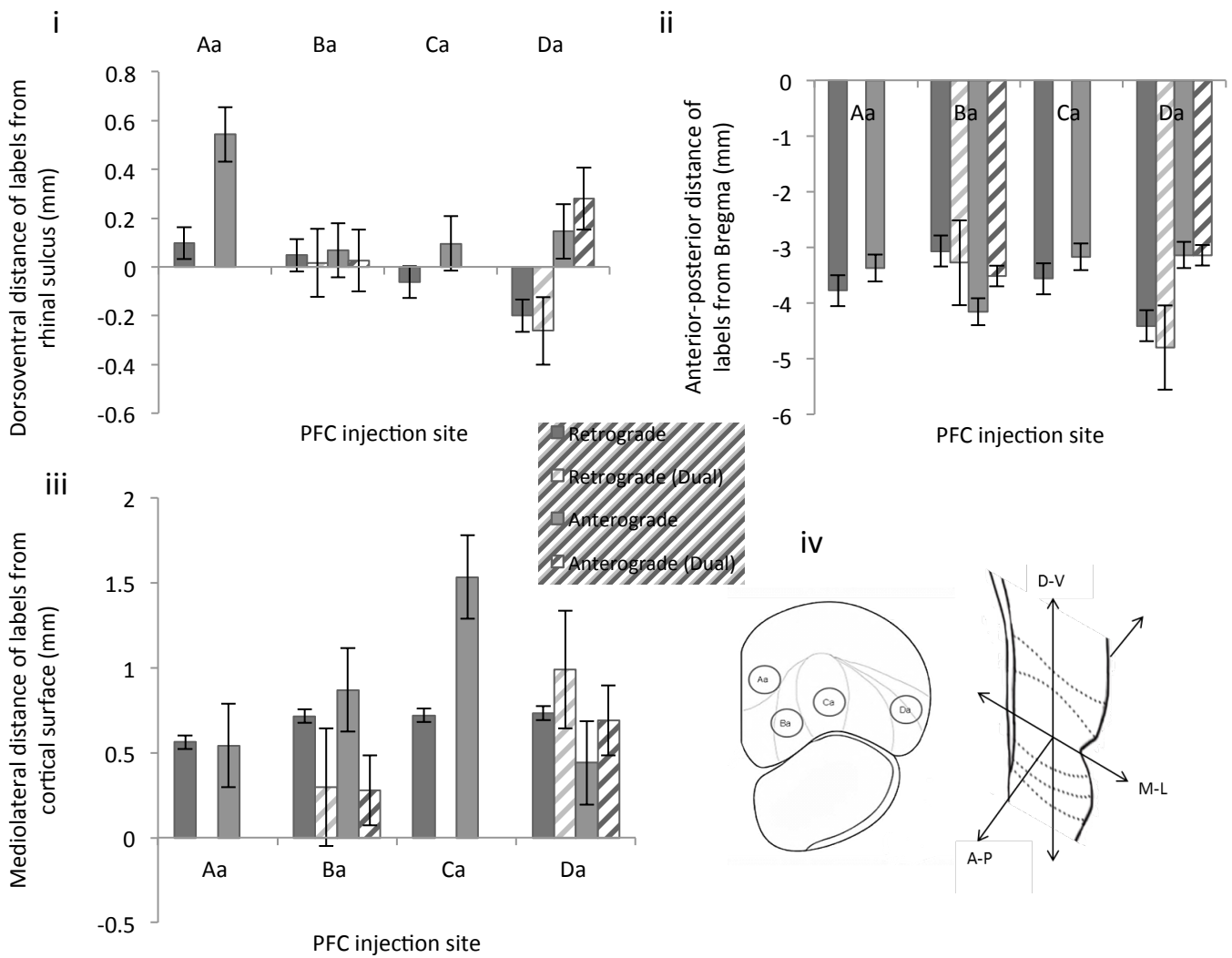


Figure 9. The mean effect of anterior PFC injection site on the location of retrograde (Aa n=75, Ba n=102 [dual injection n=157], Ca n=334, Da n=67 [dual injection n=16]) and anterograde (Aa n=47, Ba n=29 [dual injection n=224], Ca n=113, Da n=31 [dual injection n=28]) afferents and efferents in temporal cortex in (i) dorsoventral, (ii) anterior-posterior and (iii) mediolateral axes. (iv) Coronal cross section of PFC indicating the position of four injection sites within PFC: Prelimbic (injection Aa), Ventral Orbital (injection Ba), Ventrolateral Orbital (injection Ca) and Dorsal Lateral Orbital (injection Da), coronal cross section of temporal cortex, depicting the three dimensions in which the locations of labelled cells were recorded. Error bars = standard error.

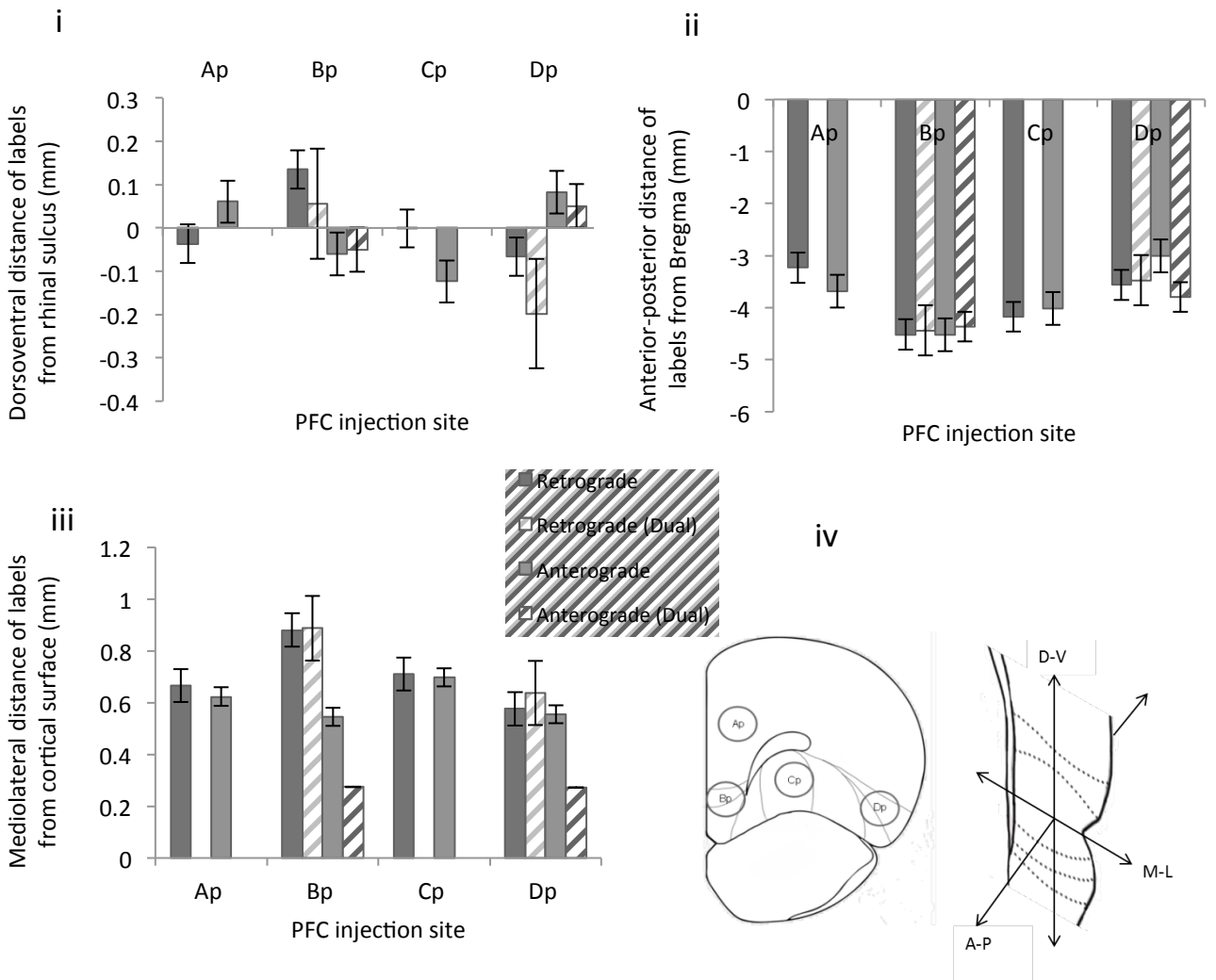


Figure 10. The mean effect of posterior PFC injection site on the location of retrograde (Ap n=114, Bp n=25 [dual injection n=159], Cp n=85, Dp n=45 [dual injection n=143]) and anterograde (Ap n=51, Bp n=36 [dual injection n=46], Cp n=113, Dp n=61 [dual injection n=213]) afferents and efferents in temporal cortex in (i) dorsoventral, (ii) anterior-posterior and (iii) mediolateral axes. (iv) Coronal cross section of PFC indicating the position of four injection sites within PFC: : PL,Cg1, M2 (injection Ap), VO,MO,IL,PL (injection Bp), VLO,M2 (injection Cp) [VLO alone in the case of the anterograde single injection] and LO,Al,DI,GI (injection Dp), coronal cross section of temporal cortex, depicting the three dimensions in which the locations of labelled cells were recorded. Error bars = standard error.

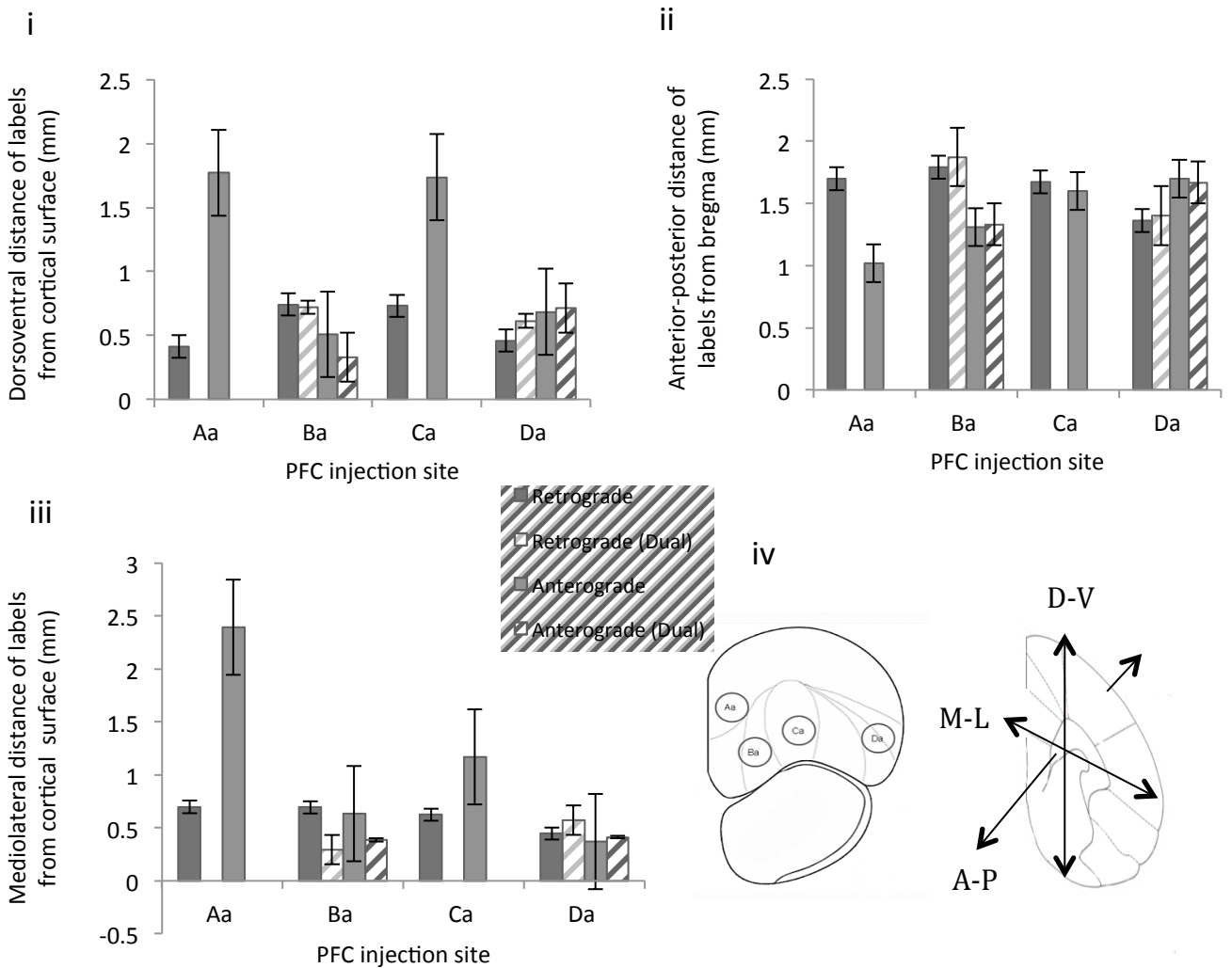


Figure 11. The mean effect of anterior PFC injection site on the location of retrograde (Aa n=20, Ba n=77 [dual injection n=313], Ca n=39, Da n=72 [dual injection n=134]) and anterograde (Aa n=87, Ba n=91 [dual injection n=322], Ca n=30, Da n=36 [dual injection n=45]) afferents and efferents in sensory-motor cortex in (i) dorsoventral, (ii) anterior-posterior and (iii) mediolateral axes. (iv) Coronal cross section of PFC indicating the position of four injection sites within PFC: Prelimbic (injection Aa), Ventral Orbital (injection Ba), Ventrolateral Orbital (injection Ca) and Dorsal Lateral Orbital (injection Da), coronal cross section of sensory-motor cortex, depicting the three dimensions in which the locations of labelled cells were recorded. Error bars = standard error.

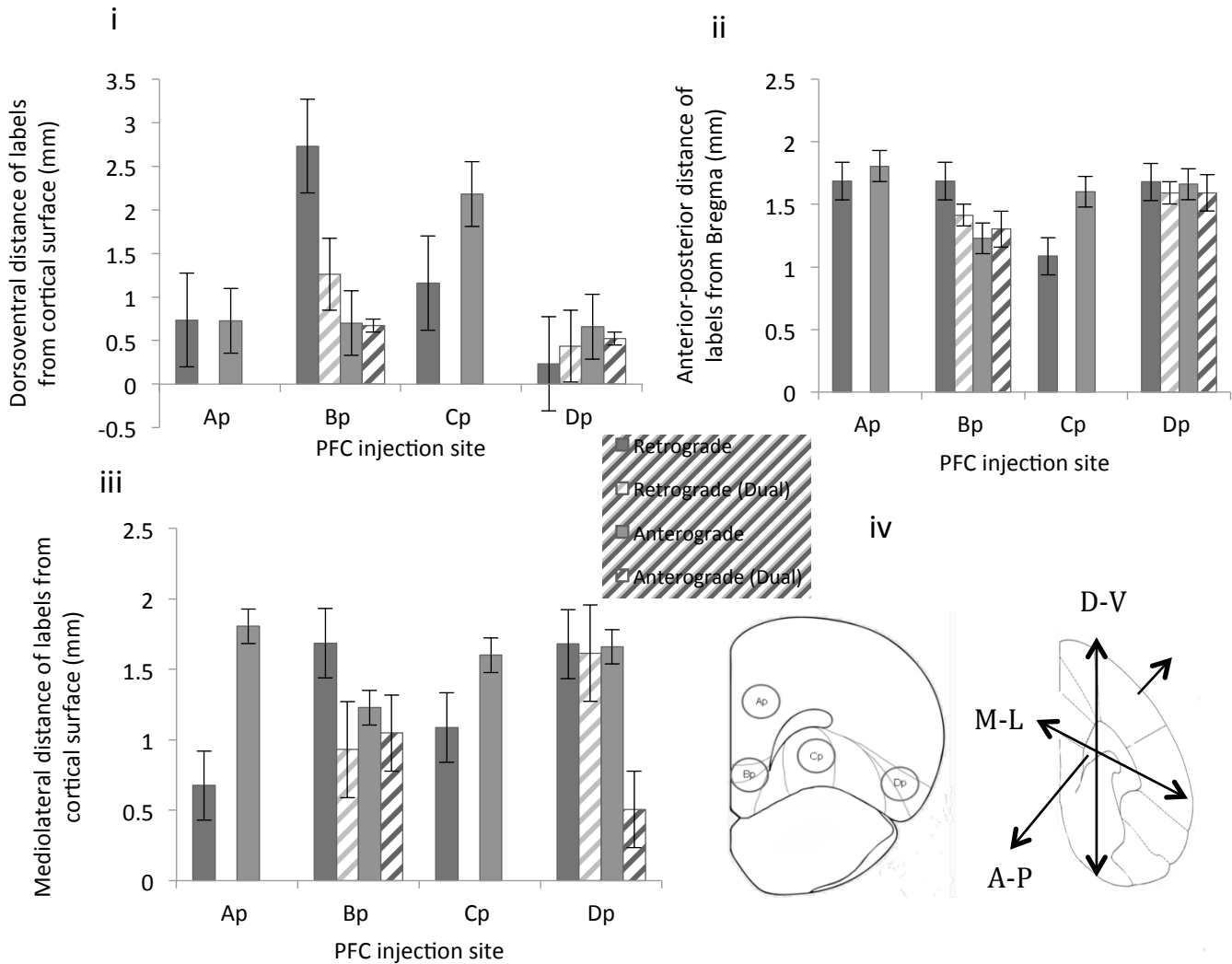
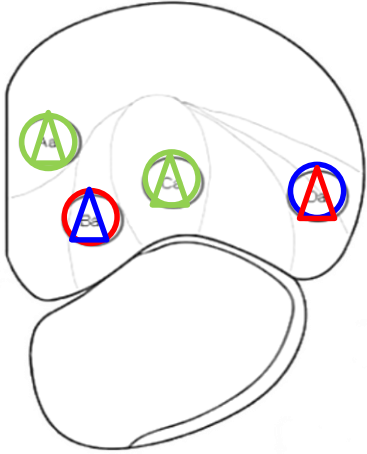
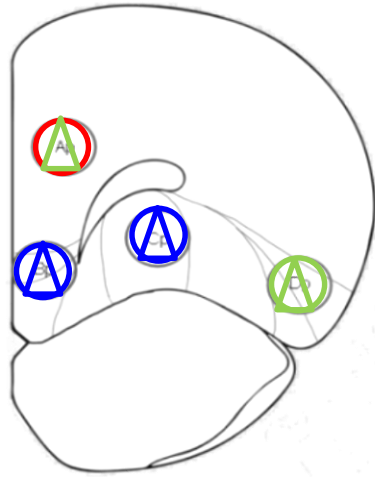


Figure 12. The mean effect of posterior PFC injection site on the location of retrograde (Ap n=152, Bp n=268 [dual injection n=168], Cp n=136, Dp n=30 [dual injection n=227]) and anterograde (Ap n=124, Bp n=44 [dual injection n=41], Cp n=35, Dp n=40 [dual injection n=29]) afferents and efferents in sensory-motor cortex in (i) dorsoventral, (ii) anterior-posterior and (iii) mediolateral axes. (iv) Coronal cross section of PFC indicating the position of four injection sites within PFC: PL,Cg1, M2 (injection Ap), VO,MO,IL,PL (injection Bp), VLO,M2 (injection Cp) [VLO alone in the case of the anterograde single injection] and LO,AI,DI,GI (injection Dp), coronal cross section of sensory-motor cortex, depicting the three dimensions in which the locations of labelled cells were recorded. Error bars = standard error.

Anterior PFC



Posterior PFC



 retrograde connections to anterior temporal cortex

 retrograde connections to central temporal cortex

 retrograde connections to posterior temporal cortex

 Anterograde connections to anterior temporal cortex

 Anterograde connections to central temporal cortex

 Anterograde connections to posterior temporal cortex